



## Review of Properties of Quark-Gluon Plasma and Ultra-Relativistic Nuclear Collisions<sup>1</sup>

LARRY MCLERRAN

*Fermi National Accelerator Laboratory*

Theoretical Physics Department

*P. O. Box 500,*

*Batavia, Illinois 60510*

### Abstract

In this talk I review current theoretical understanding of the quark-gluon plasma, and how it might be produced and detected in ultra-relativistic nuclear collisions. I first review current theoretical understanding of various possible phase changes in hadronic matter, and the asymptotic behavior of such matter at high energy density. I then discuss how the plasma might form in nuclear collisions, and what are the possible experimental probes of such a plasma. I finally briefly discuss who will do such experiments, when they will be carried out, and what experiments are planned.

---

<sup>1</sup>Talk presented at IX Workshop on High Energy Physics and Field Theory, Protvino, USSR, July 1986.



## Section 1: Introduction

The behavior of matter at high energy density has been the subject of much theoretical work in the last decade. In this talk, I will begin by briefly summarizing what is theoretically known and conjectured about the properties of high energy density hadronic matter. I will discuss the possibilities of phase changes in such matter, and the scales of energy density where this might occur.

I then turn to the much discussed issue of how high energy density matter might be formed in the collisions of ultra-relativistic nuclei, or in high multiplicity fluctuations in  $p\bar{p}$  collisions. I review the estimates of the maximum thermalized energy density which may be achieved in such collisions. I also discuss the lifetime of the system as a thermal one. Finally, I discuss evidence from experiments at Bevalac energy for collective behavior in the central collisions of large nuclei.

In the next section, I discuss proposed probes of the plasma as it might be produced. I review photons and dileptons,  $p_t$  distributions, strangeness, interferometry and jets, and discuss the semi-quantitative computations which have been done to date.

In the last section, I discuss the facilities and experiments which are being developed or have been proposed for making and experimentally studying quark-gluon plasmas.

## Section 2: The Properties of High Energy Density Hadronic Matter

In this section I shall discuss the properties of hadronic matter at high energy density. The word high implies a scale for the measurement of the energy density. Such a scale may be provided by a variety of estimates, all of which agree on the order of magnitude of a typical density scale for hadronic matter. The first is the energy density of nuclear matter. With  $m$  the proton mass,  $R_A$  the nuclear radius, and  $A$  the nuclear baryon number, the density of nuclear matter

is

$$\rho_A = \frac{Am}{\frac{4}{3}\pi R_A^3} = .14 \text{ Gev/Fm}^3 \quad (1)$$

We can also use Eq. 1 to estimate the energy density inside a proton. If we use a proton radius of .8 Fm, Eq. 1 gives

$$\rho_p = .5 \text{ Gev/Fm}^3 \quad (2)$$

There is a good deal of uncertainty in this estimate of  $\rho_p$ . We might have instead used the MIT bag radius, or a proton hard core radius, corresponding to an order of magnitude uncertainty in Eq. 2. Finally, another estimate comes from dimensional grounds using the value of the QCD  $\Lambda$  parameter, suitably defined as  $\Lambda_{\text{MS}}$  or  $\Lambda_{\text{mom}}$ , as the dimensional scale factor. Using the  $\Lambda$  parameter, we find

$$\rho_{\text{QCD}} = \Lambda^4 = .2 \text{ Gev/Fm}^3 \quad (3)$$

Again there is an order of magnitude uncertainty both due to the lack of precise experimental knowledge of  $\Lambda$ , and differences induced by using alternative sensible definitions of  $\Lambda$ .

In all of the above energy density estimates, the typical scale was in the range of several hundreds of Mev/Fm<sup>3</sup> to several Gev/Fm<sup>3</sup>. At energy densities low compared to this scale, we presumably have a low density gas of the ordinary constituents of hadronic matter, that is, mesons and nucleons. At densities very high compared to this scale, we expect an asymptotically free gas of quarks and gluons.<sup>(1)</sup> At intermediate energy densities, we expect that the properties of matter will interpolate between these dramatically different phases of matter. There may or may not be true phase changes at some intermediate densities.

To understand how such a transition might come about, consider the example of QCD in the limit of a large number of colors,  $N_c$ .<sup>(2)</sup> Recall that extensive quantities such as the energy density,  $\epsilon$ , or entropy

density,  $\sigma$ , measure the number of degrees of freedom of a system. The dimensionless quantities  $\epsilon/T^4$  or  $\sigma/T^3$  should be of the order of the number of degrees of freedom. For hadronic matter, the number of degrees of freedom relevant at low density are the number of low mass hadrons. Since matter is confined at low density, the number of such degrees of freedom is  $N_{\text{dof}} \sim 1$  in terms of the number of colors. At high energy density, the relevant number of degrees of freedom are those of unconfined quarks and gluons. The gluons dominate and give  $N_{\text{dof}} \sim N_C^2$ . Therefore in the large  $N$  limit, the number of degrees of freedom change by an infinite amount.

Assuming that the transition occurs at finite temperature in the large  $N_C$  limit, as is verified by Monte-Carlo simulation, this result can be interpreted in two ways.<sup>(3)</sup> From the vantage point of a high density world of gluons, the asymptotic energy density is finite, but at low energy density at some finite temperature the energy density goes to zero. The energy density itself is therefore an order parameter for a phase transition, and there is a limiting lowest temperature. Viewed from the low density hadronic world, there is some limiting temperature where the energy density and entropy density become infinite. Here there is a Hagedorn limiting temperature.<sup>(4)</sup>

For  $N_C = 3$ , the above statements are only approximate. The number of degrees of freedom of low mass mesons is

$$N_{\text{dof}} \sim N_F^2 \sim 4 \tag{4}$$

where we have taken the number of low mass quarks to be  $N_F \sim 2$  for the up and down quarks. The number of degrees of freedom of a quark-gluon plasma is on the other hand

$$N_{\text{dof}} \sim 40 \tag{5}$$

The number of degrees of freedom might change in a narrow temperature range, or there might be a true phase transition where the degrees of freedom change by an order of magnitude, if our speculations concerning

the large  $N_C$  limit are applicable.

Results of a Monte-Carlo simulation of the energy density are shown in Fig. 1.<sup>(5)</sup> These results are typical of the qualitative results arising from lattice Monte-Carlo simulation. The precise values of the energy density are difficult to estimate as is the scale for the temperature. The figure does make clear the essential point, on which all Monte-Carlo simulations agree, that the number of degrees of freedom of hadronic matter changes by an order of magnitude in a narrowly defined range of temperature. There is apparently a first order phase transition for SU(3) Yang-Mills theory in the absence of fermions, and a rapid transition which may or may not be a first order transition for SU(3) Yang-Mills theory with two or three flavors of massless quarks.

For Yang-Mills theory in the absence of dynamical quarks, there is a local order parameter which probes the confinement or deconfinement of a system. This order parameter measures the exponential of the free energy difference between the thermal system with and without the presence of a single static test quark inserted as a probe,

$$\langle L \rangle = e^{-\beta F_q} \quad (6)$$

As originally proposed by Polyakov<sup>(11)</sup> and Susskind,<sup>(12)</sup> and developed in Refs. (6-7), the Polyakov loop is a Wilson loop at the position of the quark which evolves only in time and is closed by virtue of the thermal boundary conditions which make the system have a finite extent in Euclidian time. The two phases of the theory are the confined and unconfined phases where

$$e^{-\beta F_q} = \begin{cases} \text{finite} & \text{unconfined} \\ 0 & \text{confined} \end{cases} \quad (7)$$

This quantity is an order parameter for a confinement-deconfinement in theories without fermions or in the large  $N_C$  limit in theories with fermions (in the fundamental representation of the gauge group). If there are fermions in the fundamental representation, in

the "confined phase" dynamical fermions may form a bound state with a heavy test quark, so the free energy is finite in what would be the confined phase.<sup>(13)</sup> Since it is already finite in the deconfined phase, the free energy of a static test quark does not provide an order parameter.

Although  $\langle L \rangle$  is not an order parameter, Monte-Carlo simulations with dynamical fermions show that  $\langle L \rangle$  changes very rapidly in a narrow range of temperatures. This is illustrated in Fig. 2 from Ref. 5, which is typical of lattice computations. For SU(3) lattice gauge theory without dynamical quarks, when  $\langle L \rangle$  is a true order parameter, there is a noticeable discontinuous change. It is not entirely clear whether there is a discontinuous change corresponding to a true phase change for the theory with fermions.

In the limit of large dynamical quark mass the quarks are no longer important at any finite temperature and decouple. In this limit the confinement-deconfinement phase transition is a well defined concept with an order parameter which measures a phase change. At zero quark masses there is another phase transition which may be carefully defined, that is, the chiral symmetry restoration phase transition. Chiral symmetry is a continuous global symmetry of the QCD lagrangian in the limit of zero quark mass. It's realization would require that all non-zero mass baryons have partners of degenerate mass and opposite parity. Since this is far from true for the spectrum of baryons observed in nature, chiral symmetry must be broken. Breaking the continuous global symmetry generates a massless Goldstone boson, which we identify with the light mass pion. As a consequence of the breaking of chiral symmetry, the quarks acquire dynamical masses, which may be seen by computing  $\langle \bar{\Psi}\Psi \rangle$ . For the chiral symmetric phase,  $\langle \bar{\Psi}\Psi \rangle = 0$ , and is non-zero in the broken phase.

For not unreasonable values of the quark masses,  $\langle \bar{\Psi}\Psi \rangle$  is plotted in Fig. 3. There appears to be a rapid change in  $\langle \bar{\Psi}\Psi \rangle$  at about the same place where the order parameter  $\langle L \rangle$  changes rapidly. We conclude therefore that chiral symmetry is approximately restored at the same

temperature where quarks stop being approximately confined. The word approximately is important here since absolute confinement or absolute chiral symmetry is impossible for finite mass dynamical quarks.

We can now conjecture on the phase diagram in the temperature mass plane. It is important to realize that we may physically vary the temperature, but not the masses of quarks. Theoretically in a Monte-Carlo simulation, these masses may be changed, but they cannot be changed in nature. It is also important to realize that the mass-temperature diagram represents an oversimplification to the case of equal mass quarks. With different mass quarks, the diagram has more variables and is more complicated.

To plot this diagram, we first discuss the limiting case  $m = \infty$ . Here there should be a first order confinement-deconfinement phase transition along the  $T$  axis. Since a discontinuous change will not be removed by a large but finite quark mass, this first order phase change must be a line of transitions in the  $m$ - $T$  plane as shown in Fig. 4. Along the  $m = 0$  axis there is a chiral symmetry restoration transition. By the arguments of Pisarski and Wilczek,<sup>(14)</sup> this transition is first order, and therefor must generate a line of transitions which extends into the  $m$ - $T$  plane.

Of course, we do not know what happens with these two lines of transitions, whether they join or never meet, or pass through one another etc. There may be no true phase transition at the values of masses which are physically relevant, or there may be one or two which are the continuation of the chiral transition from zero mass and the confinement-deconfinement transition from infinite mass. The weight of the evidence from Monte-Carlo numerical simulation suggests a very large transition in the properties of matter in a very narrow temperature range, and not much more than that can be said at present. There are a variety of conflicting claims as to whether or not there is a true first order transition at physically relevant masses.<sup>(15-20)</sup>

There have been serious attempts to obtain reliable quantitative

measures of the properties of matter from Monte-Carlo simulation.<sup>(21-22)</sup> The only truly reliable numbers have been extracted for the unphysical case of  $N_F = 0$ , that is, no dynamical fermions. It has been shown that the critical temperature of the confinement-deconfinement transition is

$$T_C = 220 \pm 50 \text{ Mev} \quad (8)$$

by fitting the potential computed in these theories and comparing it with the potential which fits charmonium. This corresponds to an energy density of 1-2 Gev/Fm<sup>3</sup> required to make a quark-gluon plasma. These results now appear to be valid for the continuum limit, and seem to be fairly good.

The numerical situation for QCD with  $N_F = 2-3$  is not nearly so good. The qualitative results have been summarized above, but it is premature to draw any firm conclusions about numbers.

### Section 3: How to Make a Quark-Gluon Plasma

The collisions of ultra-relativistic nuclei and fluctuations in  $p\bar{p}$  collisions provide the possibility of producing a quark-gluon plasma in a controlled experimental environment.<sup>(23-24)</sup> Such a collision is shown in Fig. 5 where two nuclei of transverse radius  $R$  collide in the center of mass frame. The longitudinal size of the nuclei is Lorentz contracted.

There is a scale implicit in the Lorentz contraction. Once the nuclei have a large enough Lorentz gamma factor so that they would be contracted to a size less than some typical hadronic length scale, possibly a fermi, the Lorentz contraction of virtual quanta with energy corresponding to this length scale stops. Below the beam energy appropriate for this gamma factor, the nuclei Lorentz contract. This energy is

$$E_{CM}^0 = m\gamma = m (R/l_0) = 7-70 \text{ Gev} \quad (9)$$

for uranium nuclei and the hadronic distance scale  $l_0 \sim .1 - 1$  Fm. Here and in the rest of this paper, we shall quote the center of mass energy in Gev per nucleon in each nucleus.

We expect qualitative differences in the scattering above  $E_{CM}^0$ . Another equivalent estimate of  $E_{CM}^0$  is given by estimating the energy at which the fragmentation regions of the two nuclei separate. At energies greater than  $E_{CM}^0$  there will be a central region between the two colliding nuclei, which will have small net baryon number density.

An important fact to remember about the matter formed in the collision of two ultra-relativistic nuclei is that it is born expanding in the longitudinal direction. This is because particles are formed with a more or less uniform density in rapidity. Since these particles follow a trajectory which has its origin approximately at  $x = t = 0$ , and there is a large dispersion in particle velocities, there will be a large longitudinal velocity gradient built into the initial matter distribution. There should be no transverse expansion in the initial condition since we expect a random orientation in the transverse momentum of produced particles. It can be shown that if the distribution of produced particles is uniform in rapidity, the expansion is initially a 1+1 dimensional similarity expansion, and the density of particles decreases like  $1/t$ .

The initial energy density may be estimated on dimensional grounds. The initial energy density should be proportional to the initial rapidity density per unit transverse area. The energy per particle should be of the order of the typical transverse momentum per particle. The longitudinal distance scale and  $p_t$  are correlated at early time by the uncertainty principle, since initially the matter appears in a quantum mechanical state,  $p_t \sim 1/l_0$ . We therefore have

$$\epsilon_i \sim \frac{dN}{dy} \frac{1}{\pi R^2} p_t^2 \Big|_{t=t_i} \quad (11)$$

The initial time  $t_i$  will be chosen as the earliest time we believe that

the matter may be described as approximately expanding as a perfect fluid.

If the matter expands approximately as a perfect fluid, then  $\epsilon_i$  may be bounded by parameters which are experimentally measured at late times after the matter decouples, that is, after the pions present in the late state of evolution of the matter have stopped scattering from one another, and are experimentally observed. We first use that the rapidity density in perfect fluid hydrodynamic expansion is proportional to the entropy and because entropy is conserved, one can prove that  $dN/dy$  is also conserved, at least in the central region.<sup>(25)</sup> Since the system cools as it expands,  $p_t$  is a monotonically decreasing function of time. (Some of the transverse momentum is recovered by transverse flow, but  $p_t$  nevertheless monotonically decreases.) We find therefore that

$$\epsilon_i > p_t^2 \frac{1}{\pi R^2} \frac{dN}{dy} \quad (12)$$

In this equation, all quantities are experimentally observable.

Eq. 12 may be used in combination with experimental data from the JACEE collaboration cosmic ray experiment<sup>(26)</sup> to estimate  $\epsilon_i$ . For average  $p\bar{p}$  collisions at  $E_{CM} = 100$  Gev,  $\epsilon_i = .6$  Gev/Fm<sup>3</sup>. If we take the average multiplicity for head-on collisions to be  $2A^{1/3}$  as is consistent with the JACEE results and conservatively estimate  $p_t$  as the value appropriate for  $p\bar{p}$  collisions, we find  $\epsilon_i = 10$  Gev/Fm<sup>3</sup>.

The initial energy density might be much larger than this for a variety of reasons. In fluctuations in  $p\bar{p}$  collisions, the multiplicity may be much larger. In nuclear collisions, the initial  $p_t$  may be much larger than is typical of the final state. This initial  $p_t$  may be determined by kinetic theory arguments, and might be in the range of .4 - 2 Gev,<sup>(27-28)</sup> corresponding to uncertainty in the energy density of at least an order of magnitude. The initial transverse momentum, and correspondingly, the initial time, may even depend upon the nuclear baryon number A.<sup>(29-31)</sup> I think the best estimates of the achievable

energy densities in central collisions of large nuclei is 2-200 Gev/Fm<sup>3</sup>. This corresponds to an initial temperature in the range of T<sub>i</sub> - 200-700 Mev.

Such a large uncertainty in the parameters which describe matter formed in ultra-relativistic nuclear collisions is unfortunately typical of the field, a field where there has been little experimental data. While the range of achieved energy densities seems sufficient to form a quark-gluon plasma, there is much reason for caution.

To make a convincing case that there is sufficient time for the formation and evolution of a quark-gluon plasma as an approximate perfect fluid, the expansion rate of the system should be compared to a typical particle collision time. When the collision time is much less than the expansion time, the system should expand approximately adiabatically as a perfect fluid. Since entropy is conserved, the initial and final times for expansion in d dimensions are related by

$$(t_f/t_i)^d = (\sigma_i/\sigma_f) - \frac{N_{dof}^i}{N_{dof}^f} \frac{T_i^3}{T_f^3} \sim 10-10^4 \quad (13)$$

where  $\sigma$  is the entropy density and  $N_{dof}$  are the number of particle degrees of freedom. At early time, the expansion is 1 dimensional, and later times becomes three dimensional. We estimate therefore that  $t_f/t_i \sim 10 - 10^3$ . Detailed hydrodynamic computations show that the final decoupling time is probably somewhere in the range of  $t_f \sim 20 - 50 \text{ Fm}/c$ .<sup>(32-33)</sup>

Large nuclei are clearly the more favored system for producing and studying a quark-gluon plasma. This follows simply from the facts that the average energy density achieved is larger, and that the system is physically larger in transverse extent. We require  $\lambda_{scat} \ll R_{nuc}$  in order for a perfect fluid hydrodynamic treatment to be sensible. Estimates of  $\lambda_{scat}$  give .1-1 Fm.<sup>(27-28)</sup>

Experimental data exists which throws some light on the size of systems necessary for fluid dynamic effects to become important. At

Bevalac energies, the flow of hadronic matter was studied in nuclear collisions.<sup>(34-35)</sup> In collisions of nuclei of small impact parameter, single particle collisions occur at large transverse momentum. The nuclei do not collectively flow in a given transverse direction unless there is subsequent rescatterings among the constituents of the nuclei. If these subsequent rescatterings do not occur, the transverse momentum of each particle is randomly oriented. To get collective flow, one needs rescattering, and this should be enhanced in collisions at small impact parameter, and collisions of large A nuclei.

In Fig. 6, the flow angle is plotted for various measures of the impact parameter (large impact parameters at the top and small at the bottom of the figure) for various nuclei (small on the left and large on the right). Little evidence of flow is shown for nuclei as large as calcium, and collective effects begin to become important for nuclei of the size of niobium.

#### Section 4: Probes of the Quark-Gluon Plasma

In Table I, various experimental probes of the quark-gluon plasma are presented. We shall discuss in detail these probes in this section. The bottom line on all of these probes is that they all will involve correlations between several variables. For example, just the requirement of head-on, small impact parameter collisions requires a cut either on total multiplicity or nuclear fragmentation. Because of this often times complicated analysis of correlated variables, it is difficult to argue that any one of the probes will yield an unambiguous signal for a plasma. Nevertheless, in several cases such as photon and di-lepton probes, with a little luck it may be possible to construct a convincing case that a plasma has been formed, and to measure some of its properties.

##### Sub-section 4a: Photons and Dileptons

In Fig. 7, quark-antiquark annihilation to produce di-lepton pairs is shown. If we sum over all possible quark-gluon interactions in the

initial and final state, then the overall rate for production of di-leptons and photons per unit time and volume is proportional to<sup>(36)</sup>

$$\frac{dN}{dt d^3x d^4q} \sim \text{Im} \int d^4x \langle J^\mu(x) J^\nu(0) \rangle e^{iq \cdot x} \quad (14)$$

This assumes emission from a plasma at a fixed temperature  $T$ . The brackets  $\langle \rangle$  denote a thermal expectation value. The current  $J^\mu(x)$  has a real, Minkowski time argument.

There are of course a variety of non-thermal sources for di-leptons and photons. There are backgrounds for photons from  $\pi^0$  decays, which in the low  $q$  region obscure the signal. There may also be backgrounds for the di-leptons arising from decays of charmed particles. For large  $q$ , hard scattering processes from the initially un-thermalized beams of quarks and gluons presumably dominate. As the momentum is softened, the contributions arise from an ever more thermalized system which eventually may come from a plasma, provided backgrounds from soft hadronic decays do not become too large of a background. In this intermediate range of  $q$ , there are several thermal regions which contribute. At the higher  $q$  values, there is presumably a contribution from a quark-gluon plasma, at lower  $q$  a mixed phase of plasma and hadronic gas, and at the lowest  $q$  values larger than that for which background becomes important, there is a contribution from a hadronic gas.

To compute these distributions of photons and di-leptons, a knowledge of the space-time history of the evolution of the quark-gluon plasma is required.<sup>(37-40)</sup> Detailed estimates of the space-time evolution of matter produced in head-on collisions of nuclei at large  $A$  have now been carried out,<sup>(40-43)</sup> and the di-lepton distributions have been computed in detail. There has as yet been no attempt to treat non zero impact parameter collisions. The fragmentation region might be studied by techniques used in Refs. 46-48. No attempt has been made to treat the pre-equilibrium region, although the cascade computation of Boal may be useful for this.<sup>(49)</sup> A treatment of the late stages in the evolution of the matter are best treated by cascade simulation of pion

interactions, and again could be easily be used to compute di-lepton and photon distributions.<sup>(50)</sup>

The general results of these analysis are the following:

1) For photons and di-leptons emitted from the plasma, the rapidity density of the electromagnetically produced particles is correlated with the rapidity density squared of hadrons. This has been shown to be a general feature of models where the electromagnetically produced particles are produced by final state interactions of hadrons.<sup>(51)</sup> A plot of this correlation computed in a 1+1 dimensional hydrodynamic model is shown in Fig. 8.<sup>(44)</sup>

2) Pion rapidity fluctuations are correlated with fluctuations in the di-lepton and photon production rate, at the same rapidity, for thermal emission. This correlation is much different from the case for Drell-Yan pair production where there is no such correlation.

3) The rate of thermal production may be as high as  $10^2$  times background for not unreasonable values of the temperature. The plasma contribution is most sensitive to the values of the initial temperature when the system becomes thermalized. In Figs. 9a-9b, these thermal distributions are compared to backgrounds from Drell-Yan, and a generous estimate of backgrounds from resonance other low  $p_t$  phenomenon. For an initial temperature of 500 Mev, the thermal signal is always  $10^2$  times background for masses of 2-4 Gev, as shown in Fig. 9a. For initial temperature of 240 Mev, the di-lepton spectrum is shown in Fig. 9b. Here the plasma contribution is of the same order as the Drell-Yan contribution for masses of 2-4 Gev.

4) The shape of the thermal di-lepton distribution is fairly sensitive to  $T_i$ , the largest value of the temperature for which there is a thermal distribution. The effects of a pre-equilibrium distribution of quarks and gluons has not yet been included so this conclusion is a little soft.

5) For a quark-gluon plasma at high temperature, the distribution of di-leptons is a function only of the transverse mass,  $M_t = \{M^2 + p_t^2\}^{1/2}$ . There should be a strong correlation between  $M$  and  $p_t$ , a correlation not present in the Drell-Yan distribution for intermediate mass pairs.

6) The distribution of di-leptons in no simple way reflects the transition temperature. This is a consequence of doing a proper 3+1 dimensional hydrodynamic computation. In 1+1 dimensional computations, the transition temperature controls the distribution in the region of  $M \sim 1-2$  Gev. The shape does of course weakly reflect the transition temperature, but there seems no obvious or convincing way to extract it.

7) The proposed melting of low mass resonances such as the  $\rho$  and  $\omega$ , characteristic of 1+1 dimensional hydrodynamic simulations,<sup>(52-54)</sup> is not verified in 3+1 dimensional computations. In 1+1 dimensions, the  $\rho$  and  $\omega$  disappear as a resonance in the mass spectrum at large  $p_t$  since di-leptons at large  $p_t$  are emitted from a high temperature plasma. A high temperature plasma has no  $\rho$  or  $\omega$  resonance. This effect disappears in the 3+1 dimensional computations because transverse expansion makes a large amount of rapidly expanding hadron gas. This transversely expanding hadron gas dominates the spectrum for masses of  $M \sim 1$  Gev and large  $p_t$ . The melting phenomenon is presumably still affective for large mass resonances such as the  $J/\psi$ .<sup>(55)</sup>

Sub-section 4b: The Correlation Between  $p_t$  and  $\frac{dN}{dy}$

The correlation between  $p_t$  and  $\frac{dN}{dy}$  reflects properties of the equation of state of matter.<sup>(56-57)</sup> This is easily seen from the example of a spherically expanding gas. We assume that at some initial time, there is a spherically symmetric drop of hadronic matter of uniform density matter at rest. We then allow the system to hydrodynamically expand. We assume we know the volume of the initial system,  $V_0$ . We measure the total energy of all particles and the total multiplicity of particles in the final state. Since the system is slowly expanding at

late times, the entropy of particles in the final state is known assuming the particles were produced thermally from a weakly interacting gas. Since energy and entropy are conserved in the expansion of a perfect fluid, the energy and entropy of the final state is that of the initial state. We can therefore experimentally measure the correlation between say  $p_t$ , which is proportional to  $E/S$ , and the energy density.<sup>(58-59)</sup> We can compare this to a theoretically predicted correlation determined by knowing the equation of state.

A plot of  $E/S$  verse  $\epsilon$  is shown in Fig. 10 for a bag model equation of state. The generic features of this curve are straightforward to understand. At low temperature, in the pion gas phase, and high temperatures, in the plasma phase,  $E/S \propto T$ . The energy density in these two phases goes as  $\epsilon \sim N_{\text{dof}} T^4$ . Since the number of degrees of freedom changes at the transition, there is a gap between these two curves. The gap is filled by the region where the plasma cools into a pion gas. This happens at a fixed  $T$ , and almost fixed  $E/S$ , for varying  $\epsilon$ .

There are several problems when this is applied to the more realistic expansion scenarios appropriate for central collisions of heavy nuclei. First  $p_t$  is not conserved since longitudinal expansion causes the transverse momentum of individual particles to be converted into un-observed collective flow in the longitudinal direction. A correlation between  $p_t$  and say multiplicity is therefore weaker than is the case for spherical expansion. It also depends more on the detailed numerical simulation of the hydrodynamic equations. Also, the initial conditions for the matter are not so well known. The final state decoupling and perhaps a phase change may produce some entropy. Fortunately these problems do not appear to generate much dispersion in the numerical results for such a correlation.<sup>(40)</sup> Finally, a severe limitation of present hydrodynamic simulations is that they are limited to the central region of impact parameter zero collisions. If we only have a multiplicity trigger to measure the degree to which collisions occurred at zero impact parameter, then the low multiplicity events will always be dominated by large impact parameter, and their contributions

have not been computed. The present computations may therefore only provide information on head-on collisions and their fluctuations. Since the number of particles is already large, the fractional fluctuations in the multiplicity for such head-on collisions is small.

There is also the potential problem of backgrounds from conventional processes such as mini-jets obscuring the  $p_t$  enhancement from a quark-gluon plasma.<sup>(60)</sup> At energies typical of the SPS collider, production of mini-jets is presumably responsible for the high multiplicity events. In nuclear collisions at energies less than or equal to those proposed at RHIC, mini-jets are not expected to be a large background since the beam energy is low. Moreover, mini-jets should thermalize in the high multiplicity environment typical of central collisions of large nuclei, thus changing the initial conditions by making the matter initially a little hotter, but yielding a correlation between  $p_t$  and  $dN/dy$  which may be computed by hydrodynamics.

In Fig. 11, the results of a hydrodynamic computation of  $p_t$  vs  $dN/dy$  is shown for an equation of state typical of the bag model and a pion gas equation of state. The difference between these curves is large suggesting that an experimental probe of this correlation can resolve various equations of state. A general feature is that the softer is the equation of state, the softer is the  $p_t$ . A quark-gluon plasma produces lower  $p_t$  particles at fixed multiplicity than does a pion gas.

In Fig. 12, the same correlation is shown for head-on collisions of various nuclei. The curves approximately scale as a function of  $\frac{1}{A} \frac{dN}{dy}$ . The factor of  $\frac{1}{A^{2/3}} \frac{dN}{dy}$  arises because the result must be proportional to the multiplicity per unit area. An additional suppression by a factor of  $A^{1/3}$  arises due to the softening effects of longitudinal expansion.

As had been argued by Shuryak,<sup>(56)</sup> heavy particles should show the effect of collective transverse expansion more strongly than do light particles. This is shown in Fig. 13 where  $p_t$  is computed for pions

kaons and nucleons as a function of multiplicity. The physical origin of this effect is that in fluid expansion, there is a collective fluid velocity. Heavier particles have larger masses and therefore  $p = mv$  is correspondingly larger.

In Fig. 14, the  $p_t$  distributions of pions, kaons and nucleons are shown. The distribution of nucleons clearly shows the effects of collective flow with the local maximum in  $dN/d^2p_t$  at  $p_t \sim 1\text{Gev}$ .

In Fig. 12, an attempt is made to fit the experimentally observed correlation between  $p_t$  and transverse energy per unit rapidity as seen in the JACEE collaboration.<sup>(26)</sup> The JACEE data rises too rapidly to be explained by a quark-gluon plasma. The data does seem to be fit by a pion gas model (dashed line), but the temperatures where the system would be required to be in an ideal pion gas are quite large, and we consider this explanation unlikely. Either there is some non-thermal source of high  $p_t$  particles in the JACEE data, something is wrong with the space-time picture of the collisions,<sup>(58)</sup> or something is wrong with the data analysis.

#### Sub-section 4c: Strange Particle Production.

Strangeness has been widely suggested as a possible signal for the production of a quark-gluon plasma.<sup>(61-62)</sup> The argument for large strangeness in its most naive form follows from the observation that there are equal numbers of up, down and strange quarks in the plasma. One might naively expect that there would be roughly equal numbers of kaons and pions produced, and that the ratio of strange to non-strange baryons would be proportional to their statistical weight,  $N_S/N_{NS} \sim 2/3$ .

For the case of mesons, the above argument may be easily seen to be false.<sup>(63-64)</sup> In the expansion of the quark-gluon plasma, and later the hadron gas, entropy is conserved, and the pions are a result of this entropy. A better measure of the strangeness of a plasma is therefore the  $K/S$  ratio, where  $S$  is the entropy. This may be computed and shown to be smaller in a plasma than in a hadron gas for all temperatures

larger than 100 Mev. The  $K/\pi$  ratio is therefore not a direct signal for a plasma. Further, the  $K/\pi$  ratio may be computed in a variety of hydrodynamic scenarios.<sup>(64-67)</sup> The result is typically  $K/\pi \sim .3$ . This number is a little larger than is typical of pp interactions. As has been suggested by Rafelski and Muller, perhaps only if a plasma is formed will the dynamics allow for such a large  $K/\pi$  ratio, and therefore is a signal of interesting dynamics, or perhaps even the production of a plasma.<sup>(68)</sup>

Strange baryons and anti-baryons may also provide a signal. Direct computations of the ratio of the ratios of strange to non-strange baryons in a plasma to that in a hadronic gas shows however that a hadronic gas is (if at all) only a little less strange than a plasma.<sup>(63,69)</sup> These estimates are done for net baryon number zero plasma, and an enhancement may exist for the plasma in the baryon number rich region. At RHIC and SPS energies, the baryon number density is effectively small at all rapidities, and this should be a good approximation. Again, although this ratio of ratios indicates a lack of a signal for equilibrium quark-gluon plasmas, the ratio of non-strange to strange baryons is large,  $.3-2$ , in either scenario for  $100 \text{ Mev} < T < 300 \text{ Mev}$ . This number is far larger than is typical of pp interactions, and again by the arguments of Rafelski and Muller, perhaps the only way to dynamically achieve this is by production of the plasma.<sup>(68)</sup> This ratio is therefore interesting for dynamical reasons.

I conclude therefore that a large strangeness signal is not a direct signal for production of a quark-gluon plasma. It is almost certainly a signal for interesting dynamics, and it may be true that the only reasonable dynamical scenarios where large strangeness may be produced involve the formation of a quark-gluon plasma.

#### Sub-section 4d: Hanberry-Brown-Twiss

The Hanberry-Brown-Twiss effect arises from the interference of the matter waves of identical particles as they are measured in coin-

cidence experiments. In Fig 16, the two possible paths of particles from emission to two coincidence detectors are shown. If the amplitudes for this process are summed and squared, even for incoherent emission amplitudes, the result depends on the distance of separation of the emission regions. For relative particle momentum  $k \lesssim R^{-1}$ , the detection probability is modified from its incoherent form.

The measurement of identical particles closely correlated in momentum therefore allows the possibility of measuring properties of the space-time evolution of matter produced in heavy ion collisions.<sup>(70-72)</sup> One can in principle measure the size and shape of the matter at the temperature when decoupling occurs, and perhaps verify the existence of an inside-outside cascade description.

The theoretical predictions of the Hanberry-Brown-Twiss correlation are complicated by a variety of factors. The interference may be obscured by final state hadronic interactions which are difficult to compute. The space-time profile of decoupling is not yet so well known, and depends on details of the hydrodynamic simulations as well as the details of decoupling. Assuming that decoupling occurs at late times and large transverse sizes,  $t, r_t \gtrsim R$ , the correlation occurs only for very small relative momentum, and is very difficult to measure.

#### Sub-section 4e: Jets

The rescattering of jets after production in a quark-gluon plasma in principle provides a probe of the plasma and hadronic matter as the jet plows through the evolving system.<sup>(73-75)</sup> The jets will scatter from the constituents of the plasma as well as the constituents of hadronic matter which forms later. The degree of scattering is a measure of the quark-matter or gluon-matter cross section.

This scattering can dramatically change quantities such as the jet acoplanarity, and can produce phenomenon such as single jets. Theoretical predictions of jet acoplanarity for a variety of jet  $p_t$  for

an  $A = 100$  nucleus are shown in Fig. 17. The dashed curve represents the theoretical prediction in the absence of a hadronic matter distribution. The solid line includes rescattering. For jets of mass 10 Gev, the difference is striking, and the rescattering removes the planar nature of the jets. Even at jet mass of 20 Gev, the difference is still significant, and the jets are remarkably planar. In fact at these masses, the jets are probably largely extinguished.

The experimental measurement of this acoplanarity is very difficult. Particles with low rapidities along the jet axis,  $y < 2$ , must be somehow removed from the sample of particles contributing to the acoplanarity distribution. These low  $p_t$  particles arise from conventional low  $p_t$  processes, and have little in common with the high  $p_t$  particles associated with the jet.

#### Section 5 Who, What and When.

There are a variety of proposed and existing relativistic heavy ion machines where experiments of one sort or another might be done. In Fig. 18, the rapidity gap produced in such machines is plotted against allowed center of mass energy.<sup>(76)</sup> (On this plot, the proposed ITEP machine is not included. This machine falls a little above the synchrotron.) The AGS, RHIC and the SPS are the only machines where a reasonably large rapidity gap may be accessed. The RHIC is the only machine which may achieve truly asymptotic energies where a central region opens up.

In addition to beam energy, an important factor for these machines is the  $A$  of nuclei which will be accelerated. The AGS in the near future, and the SPS for the foreseeable future will accelerate light ions. In view of the Bevalac data on flow angles, this may be a dangerous thing to do. The collisions at the SPS and the AGS can involve light nuclei on heavy targets, but this considerably complicates any theoretical analysis. Perhaps some hint of the formation of a quark-gluon plasma may be extracted from such collisions, or if there is much good luck, a compelling case. A more

important concern is however to see what can and cannot be measured in the dirty experimental environment provided by ultra-relativistic nuclear collisions.

In Table II, the number of experiments and number of experimentalists involved is shown for the experimental programs at the SPS and the AGS.<sup>(76)</sup> There are 5 major experiments which will analyze heavy ion collisions at the SPS and 12 experiments at the AGS. About 159 physicists are involved in the AGS program, and 208 at the SPS. The nuclear experimentalists outnumber the high energy by 235 to 132, but there is nevertheless a large commitment from both communities.

Not shown in Fig 18, or listed in Table II is the experimental work done at FNAL. The experiment C0 is a dedicated quark-gluon plasma experiment at the Tevatron, involving 27 people.<sup>(77)</sup> There will also be a small effort with CDF and perhaps D0 to look at high multiplicity, soft processes. These experiments are to be done at very high energy, and of course only with  $p\bar{p}$  collisions. The emphasis will be on high multiplicity fluctuations in these collisions, where almost nothing is known about collective effects, or the degree of applicability of a hydrodynamical description.

Ultra-relativistic nuclear physics begins at the AGS and SPS with light ions in the fall of 1986. By 1989, the AGS with a booster should be able to accelerate heavy ions, such as gold. The RHIC project at BNL has RandD money as of 1986.

The largest experiments at the AGS are E802, E810 and E814.<sup>(78)</sup> E802 will measure inclusive cross sections with full particle identification over a complete kinematic range, with global event trigger. E810 will measure global properties of events. E814 will measure fragmentation with global event triggers.

At the SPS, the major experiments are NA38, NA35, NA36, WA80 and NA34.<sup>(79)</sup> NA38 is a muon pair experiment. NA35 has a  $4\pi$  calorimeter and a  $2\pi$  streamer chamber. NA36 involves a TPC and  $2\pi$  calorimeter. NA34

has a  $4\pi$  calorimeter, an external spectrometer, and will measure photons and muon pairs.

At FNAL, CO will measure multiplicity in the central region, inclusive cross sections and has particle identification over a wide kinematic range.

References:

- 1) J. C. Collins and M. Perry, Phys. Rev. Lett. 34, 1353 (1975).
- 2) C. Thorn, Phys. Lett. 99B, 458 (1981).
- 3) S. R. Das and J. Kogut, Phys. Rev. D31, 2704 (1985).
- 4) R. Hagedorn, Proc. of Quark Matter 84, p 53, Edited by K. Kajantie, Springer-Verlag (1985).
- 5) T. Celik, J. Engels and H. Satz, Phys. Lett. 133B, 427 (1983); Nuc. Phys. B256, 670 (1985).
- 6) L. McLerran and B. Svetitsky, Phys. Lett. 98B, 195 (1981), Phys. Rev. D24, 450 (1981).
- 7) J. Kuti, J. Polonyi, and K. Szlachanyi, Phys. Lett. 98B, 199 (1981).
- 8) K. Kajantie, C. Montonen and E. Pietarinen, Zeit. Phys. C9, 253 (1981).
- 9) J. Engels, F. Karsch, I. Montvay and H. Satz, Phys. Lett. 101B, 89 (1981); Nuc. Phys. B205, 545 (1982).
- 10) T. Celik, J. Engels, and H. Satz, Phys. Lett. 125B, 411 (1983); Phys. Lett. 129B, 323 (1983).
- 11) A. M. Polyakov, Phys. Lett. 72B, 427 (1978).
- 12) L. Susskind, Phys. Rev. D20, 2610 (1979).
- 13) E. Fradkin and S. Shankar, Phys. Rev. D19, 3682 (1979).
- 14) R. D. Pisarski and F. Wilczek, Phys. Rev. D29, 338 (1984).
- 15) F. Fucito, and S. Solomon, Phys. Lett. 140B, 381 (1984); Phys. Rev. Lett. 55, 2641 (1985).
- 16) F. Fucito, C. Rebbi, and S. Solomon, Nuc. Phys. B248, 615 (1984); Phys. Rev. D31, 1460 (1985).
- 17) R. Gavai, M. Lev and B. Petersson, Phys. Lett. 140B, 397 (1984); Phys. Lett. 149B, 492 (1984).
- 18) M. Fukugita, S. Ohta, & A. Ukawa, Phys. Rev. Lett. 57, 503 (1986); R. Gupta, G. Guralnik, G. Kilcup and A. Patel, Los Alamos Preprint LA-UR-86-3054 (1986).
- 19) J. Kogut, J. Polonyi, H. Wyld and D. Sinclair, Nuc. Phys. B265, 293 (1986); Phys. Rev. Lett. 54, 1475 (1985).
- 20) R. Gavai and F. Karsch, Nuc. Phys. B261, 273 (1985).
- 21) A. Kennedy, B. J. Pendleton, J. Kuti and K. S. Meyer, Phys.

Lett. 155B, 414 (1985).

22) N. Christ and A. Terrano, Phys. Rev. Lett. 56, 111 (1986).

23) J. Bjorken, Lectures at the DESY Summer Institute, (1975).  
Proceedings edited by J. G. Korner, G. Kramer, and D. Schildnecht  
(Springer, Berlin, 1976).

24) R. Anishetty, P. Koehler and L. McLerran, Phys. Rev. D22,  
2793 (1980); L. McLerran, Proc. of 5th High Energy Heavy Ion Study,  
Berkeley, Ca. (1981).

25) J. Bjorken, Phys. Rev. D27, 140 (1983).

26) T. Burnett et. al., Phys. Rev. Lett. 50, 2062 (1983).

27) A. Hosoya and K. Kajantie, Nuc. Phys. B250, 666 (1985).

28) P. Danielowicz and M. Gyulassy, Phys. Rev. D31, 53 (1985).

29) H. von Gersdorff, L. McLerran, M. Kataja, and P. V. Ruuskanen,  
Phys. Rev. D34, 794 (1986).

30) A. Kerman, T. Matsui, and B. Svetitsky, Phys. Rev. Lett. 56,  
219 (1986).

31) M. Gyulassy and A. Iwazaki, LBL Preprint LBL-20318 (1985).

32) G. Baym, B. Friman, J.-P. Blaizot, M. Soyeur and W. Czyz,  
Nucl. Phys. A407, 541 (1983)

33) A. Bialas and W. Czyz, Acta. Phys. Pol. B15, 229 (1984).

34) G. Buchwald, G. Graebner, J. Theis, S. Maruhn, W. Greiner and  
H. Stocker, Phys. Rev. Lett. 52, 1594 (1984); Nucl. Phys. A418, 625  
(1984).

35) H. A. Gustafsson et. al. Phys. Rev. Lett. 52, 1590 (1984).

36) E. L. Feinberg, Nuovo. Cim. 34A, 391 (1976).

37) E. V. Shuryak and O. Zhironov, Yadern. Fiz. 24, 195 (1976);  
E. V. Shuryak, Phys. Lett. 78B, 150 (1978); E. V. Shuryak; Sov. J.  
Nuc. Phys. 28, 408 (1978).

38) L. McLerran and T. Toimela, Phys. Rev. D31, 545 (1985).

39) R. Hwa and K. Kajantie, Phys. Rev. D32, 1109 (1985).

40) H. von Gersdorff, L. McLerran, M. Kataja, and P. V.  
Ruuskanen, FNAL Preprint Fermilab-Pub-86/73T (1986).

41) B. Friman, K. Kajantie and P. V. Ruuskanen, Nucl. Phys.  
B266, 468 (1986).

42) J. P. Blaizot and J. Y. Ollitrault, Saclay Preprint (1986).

43) O. D. Chernavskaya and D. C. Chernavskaya, Kiev Preprint

ITP-86-66 (1986).

44) K. Kajantie, J. Kapusta, L. McLerran, and A. Mekjian, U. of Minn. Preprint Print-86-0414 (1986).

45) K. Kajantie, M. Kataja, L. McLerran, and P. V. Ruuskanen, Phys. Rev. D34, 811 (1986).

46) K. Kajantie and L. McLerran, Phys. Lett. 119B, 203 (1982); Nucl. Phys. B214, 261 (1983).

47) K. Kajantie, R. Raitio and P. V. Ruuskanen, Nucl. Phys. B222, 152 (1983).

48) L. Csernai and M. Gyulassy LBL Preprint (1986).

49) D. Boal, Proceedings of BNL RHIC Workshop, p. 349 (1985).

50) G. Bertsch, L. McLerran, P. V. Ruuskanen, and E. Saarkinen (in preparation).

51) J. Pisut, Proceedings of 25'th Crakow School of Theoretical Physics, Zakopane, Poland (1985); V. Csernai, P. Lichard, and J. Pisut, Z. Phys. C31, 163 (1986).

52) R. Pisarski, Phys. Lett. 110B, 1551 (1982).

53) A. I. Bochkarov and M. E. Shaposhnikov, Nuc. Phys. B268, 220 (1986).

54) P. Siemans and S. A. Chiu, Phys. Rev. Lett. 55, 1266 (1986).

55) T. Matsui and H. Satz, BNL Preprint BNL-38344 (1986).

56) E. V. Shuryak and O. Zhironov, Phys. Lett. 89B, 253 (1979); Yadern. Fiz. 21, 861 (1975).

57) L. van Hove, Phys. Lett. 118B, 138 (1982).

58) H. von Gersdorff, J. Kapusta, L. McLerran and S. Pratt, Phys. Lett. 163B, 253 (1985).

59) K. Redlich and H. Satz, Phys. Rev. D33, 3747 (1986).

60) J. C. Collins, SSC Workshop, Los Angeles (1986).

61) T. Biro, H. Barz, B. Lukacs and J. Zimanyi, Nuc. Phys. A386, 617, (1982).

62) B. Muller and J. Rafelski, Phys. Rev. Lett. 48, 1066 (1982).

63) K. Redlich, Z. Phys. C27, 633 (1985).

64) N. Glendenning and J. Rafelski, Phys. Rev. C31, 823 (1985).

65) J. Kapusta and A. Mekjian, Phys. Rev. D33, 1304 (1986).

66) T. Matsui, L. McLerran, and B. Svetitsky, Phys. Rev. D34, 783 (1986); MIT preprint MIT-CTP-1344 (1986).

- 67) K. Kajantie, M. Kataja and P. V. Ruuskanen, Jyvaskyla preprint, JYFL-9/86.
- 68) J. Rafelski and B. Muller, GSI Preprint GSI-86-7 (1986).
- 69) L. McLerran, Proceedings of Quark-Matter 86, Asilomar, Ca. (1986).
- 70) M. Gyulassy, S. Kauffmann, and L. W. Wilson, Phys. Rev. C20, 2267 (1979).
- 71) S. Pratt, Phys. Rev. Lett. 53, 1219 (1984).
- 72) W. A. Zajc, Proceedings of RHIC Workshop, BNL-51921.
- 73) J. D. Bjorken, FNAL Preprint, Fermilab-Pub-82159-T (1982).
- 74) D. Appel, Phys. Rev. D33, 717 (1986).
- 75) J. P. Blaizot and L. McLerran, FNAL preprint Fermilab-Pub-86/56-T (1986).
- 76) T. Ludlam, Proceedings of 23'rd Int. Conf. on High Energy Physics, Berkeley Ca., USA, (1986).
- 77) C. Hojvat Proceedings of 23'rd Int. Conf. on High Energy Physics, Berkeley Ca., USA, (1986).
- 78) R. Ledoux, Proceedings of 23'rd Int. Conf. on High Energy Physics, Berkeley Ca., USA, (1986).
- 79) D. Lissauer, Proceedings of 23'rd Int. Conf. on High Energy Physics, Berkeley Ca., USA, (1986).

Table I

Probes of the Quark-Gluon Plasma

Probe	Physics
Photons and Di-Leptons	$T_i$ , $T_{PT}$ , Plasma expansion, impact parameter meter, resonance
$p_t$ distributions	Equation of state, Evidence of collective fluid flow
Strangeness	Dynamics of Expansion
Pion Correlations	Size and Lifetime of plasma
Jets	Scattering cross section of quarks or gluons with plasma and hadronic matter

Table II

People

	BNL AGS	CERN SPS	TOTAL
No. Experiments	12	5	17
Total Physicists	159	208	367
University	93	115	208
Lab	66	93	159
High Energy	23	109	132
Nuclear	136	99	235
US	99	71	170
Non-US	60	140	200

Figure Captions:

- 1) Energy density scaled by  $T^4$  as a function of  $T$ .
- 2) Exponential of free energy of isolated static quark as a function of  $T$ .
- 3)  $\bar{\Psi}\Psi$  and free energy of isolated quark as function of  $T$ .
- 4) Phase diagram of QCD in the  $T$ - $m$  plane Figure 4a represents a world where the chiral and confinement phase transitions are separate, and Fig 4b is when they may be identified.
- 5) AA collision in the center of mass frame.
- 6) Flow distributions as measured by Gustafsson et. al.
- 7) Quark anti-quark annihilation to make a di-lepton pair.
- 8)  $dN/dy$  of dileptons scaled by  $dn/dy^2$  of hadrons for head-on AA collisions as function of  $dn/dy$  of hadrons.
- 9) Di-leptons in ultra-relativistic AA collisions as a function of mass of di-lepton pair. Fig. 9a is for and initial temperature of 500 Mev, and Fig. 9b is for 250 Mev.
- 10)  $E/S$  vs  $\epsilon$  in the MIT Bag Model.
- 11)  $p_t$  vs multiplicity in head on heavy ion collisions for an ideal gas equation of state (upper curve) and a bag model (lower curve).
- 12)  $p_t$  vs  $dn/dy$  scaled by  $1/A$  for a variety of  $A$ .
- 13)  $p_t$  vs  $dn/dy$  for a variety of particles.
- 14)  $p_t$  distributions for a variety of particles at a typical rapidity value.
- 15) An attempt to fit the JACEE cosmic ray data with a bag model and ideal gas equation of state.
- 16) The paths which two particles may take to coincidence detectors. The interference of the amplitudes for these two paths yields the Hanberry-Brown-Twiss correlation.
- 17) Acoplanarity distributions for jets in head on  $A=100$  collisions.  $Q= 10$  Gev in a),  $20$  Gev in b) and  $40$  Gev in c).
- 18) Center of mass energy per nucleon vs center of mass rapidity of various heavy ion accelerators.

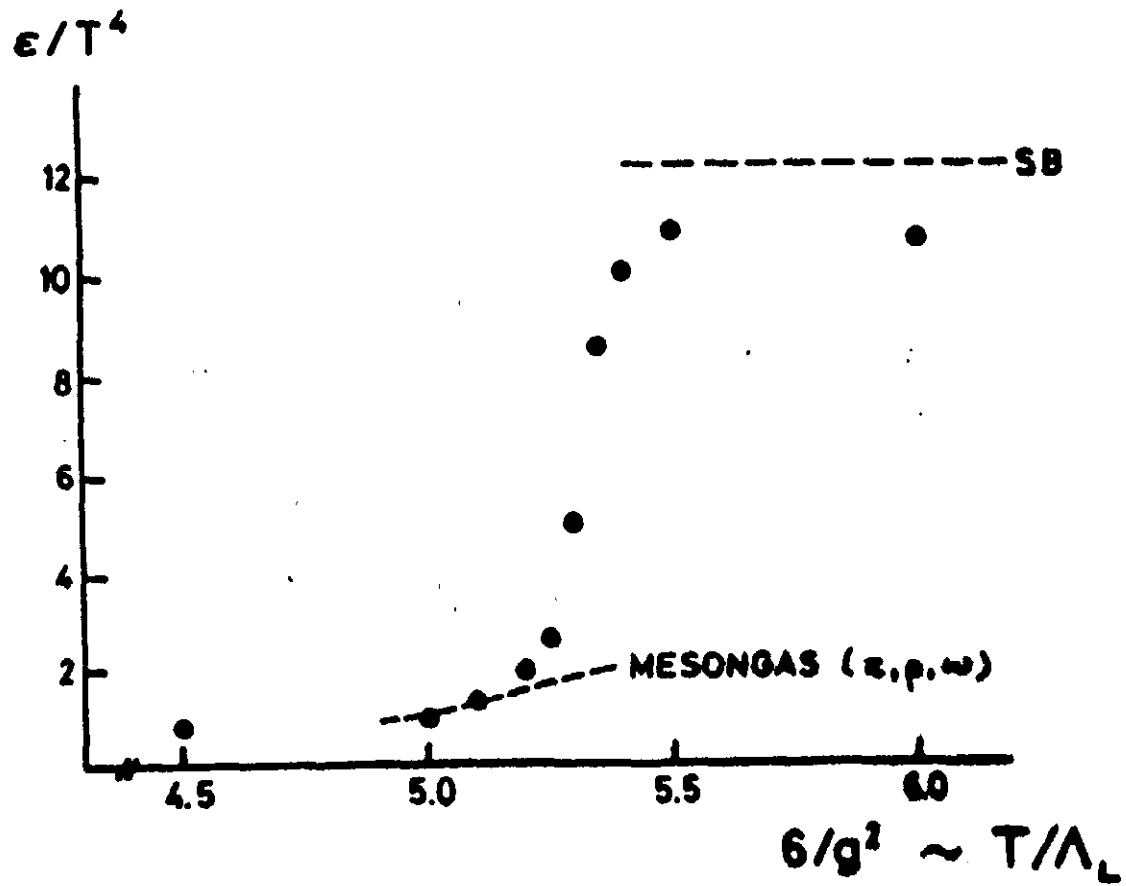


FIGURE 1

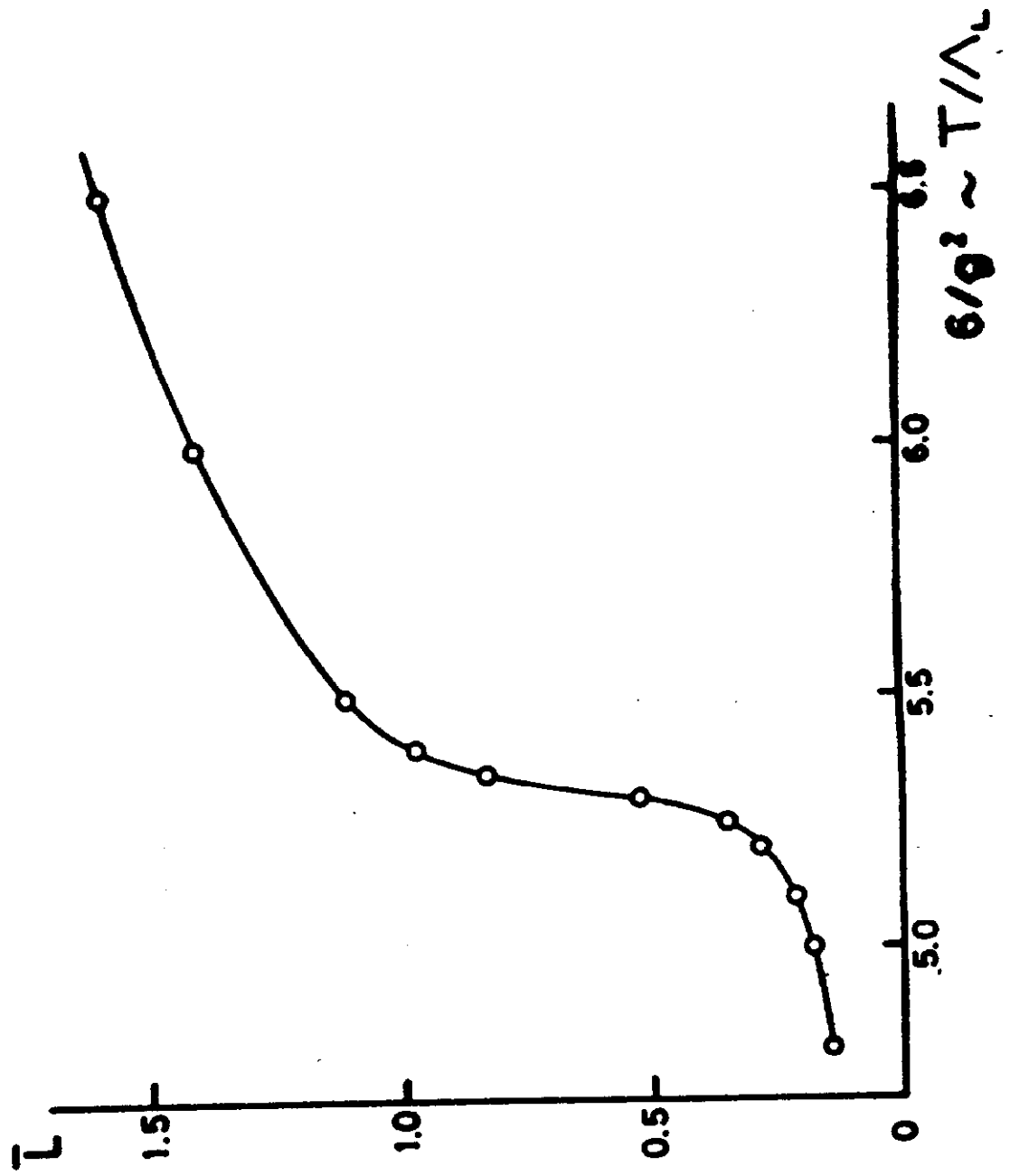


FIGURE 2

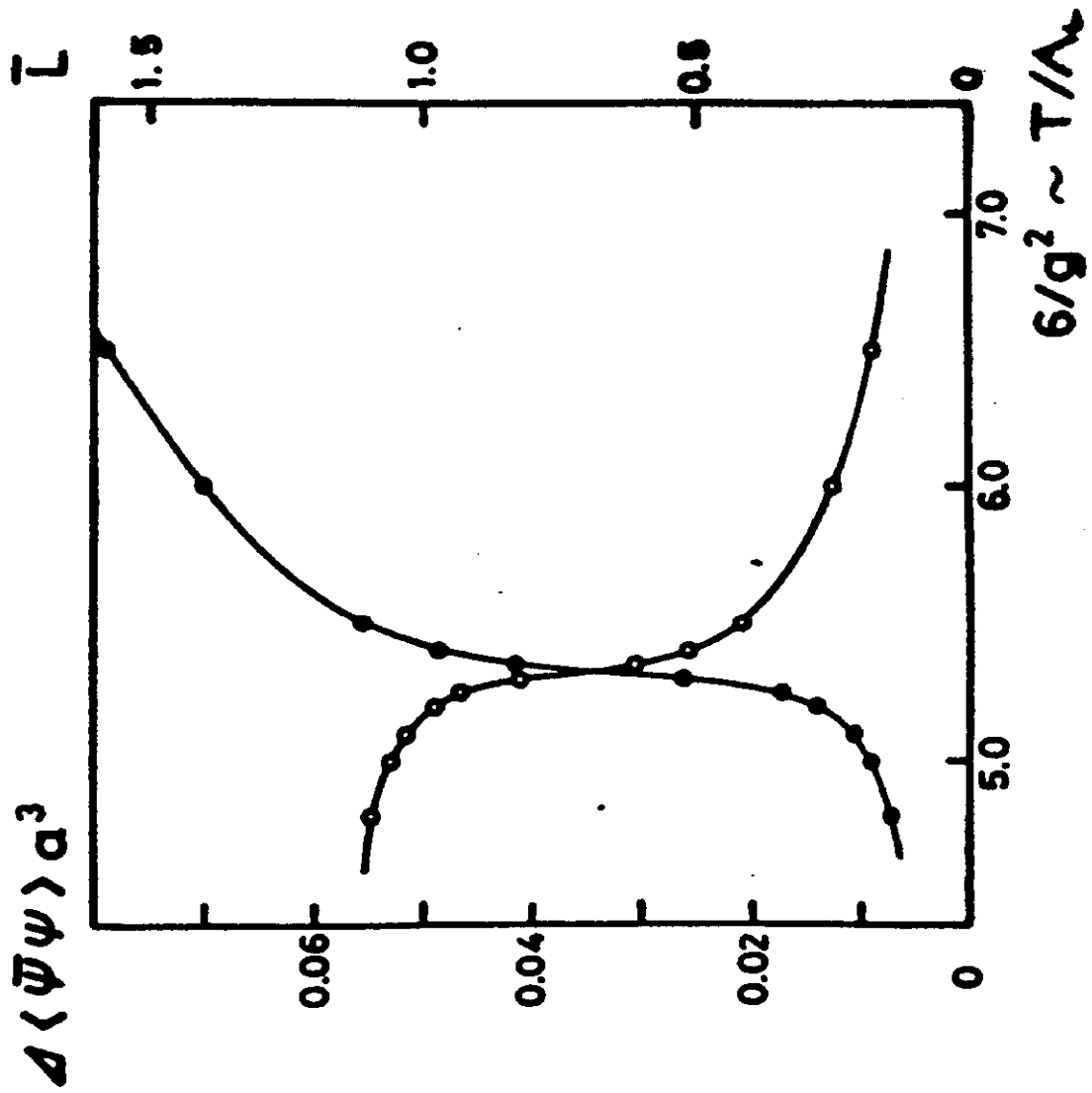


FIGURE 3

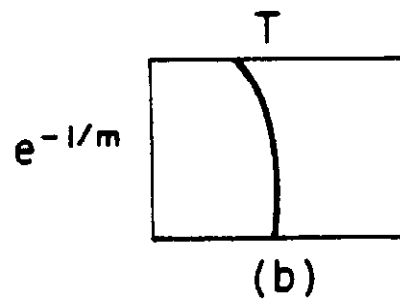
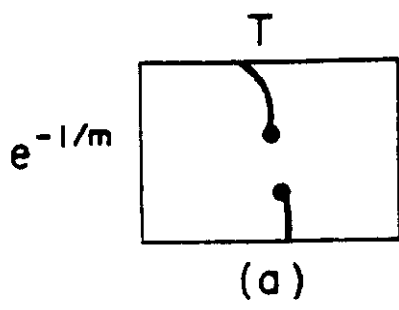


FIGURE 4

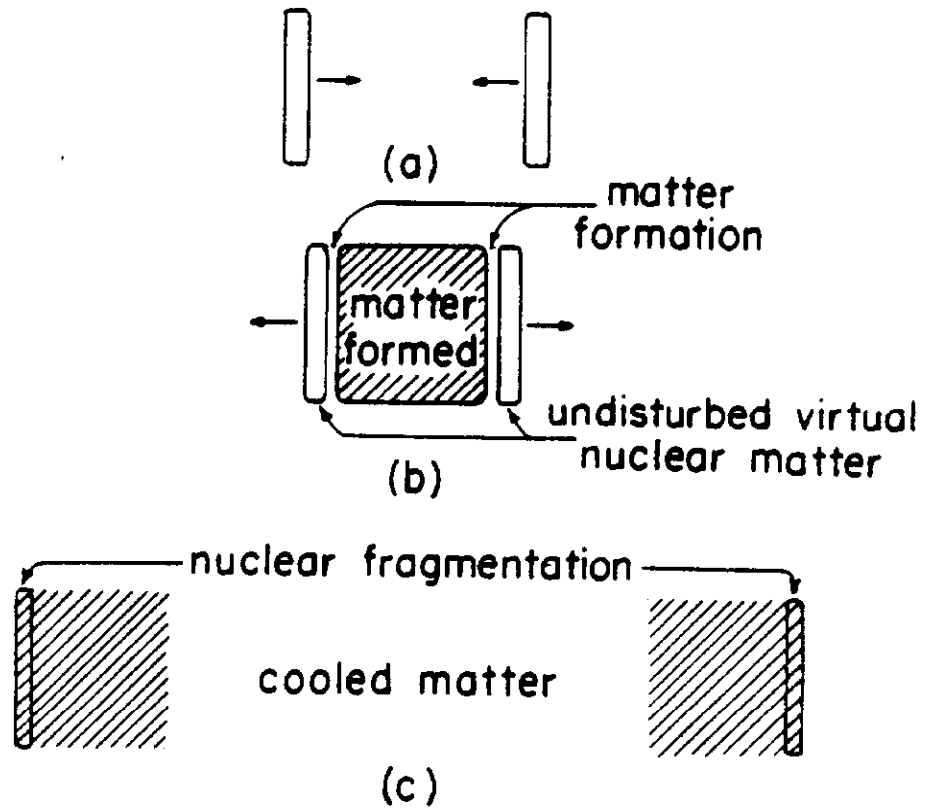


FIGURE 5

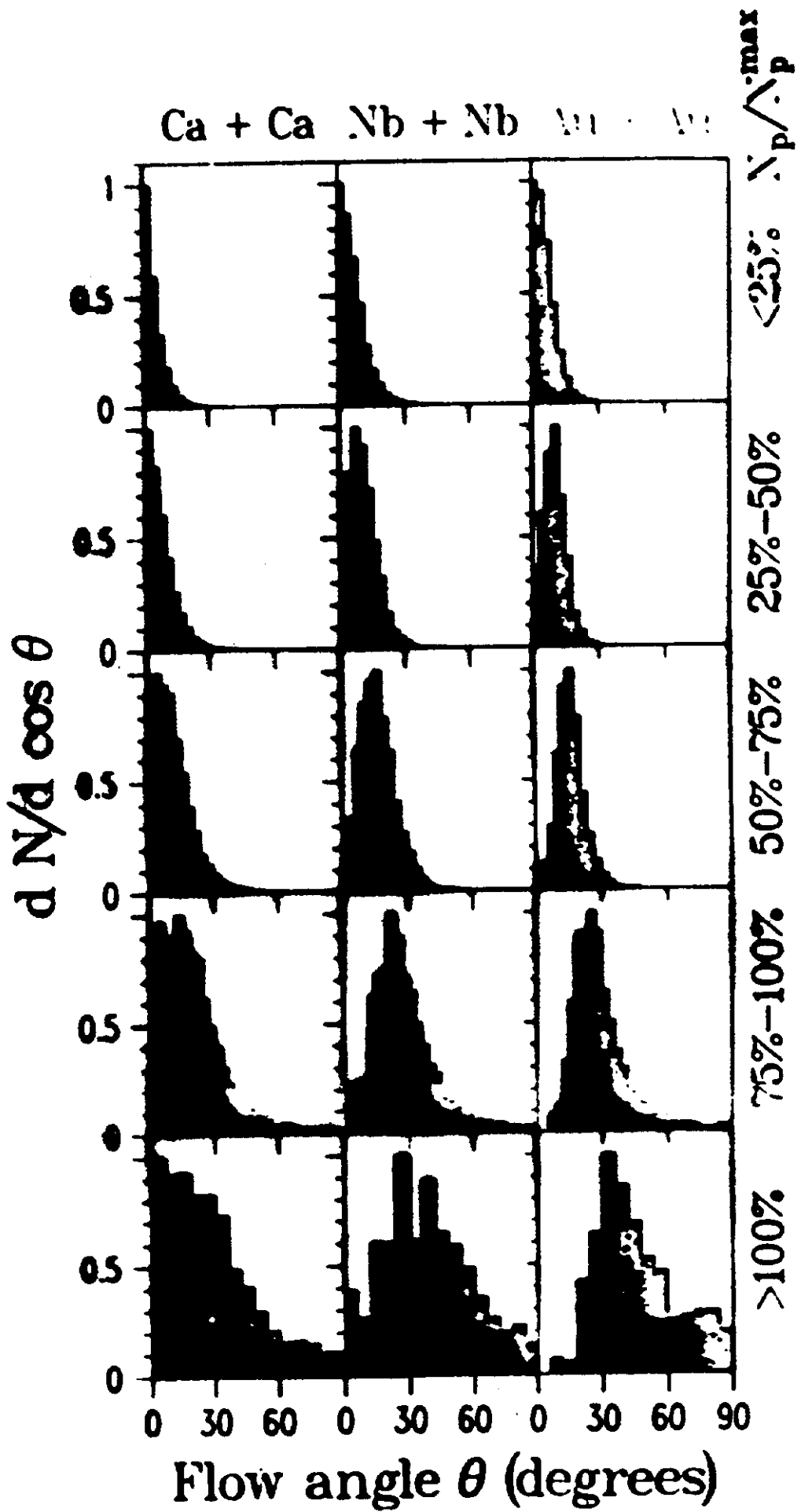


FIGURE 6

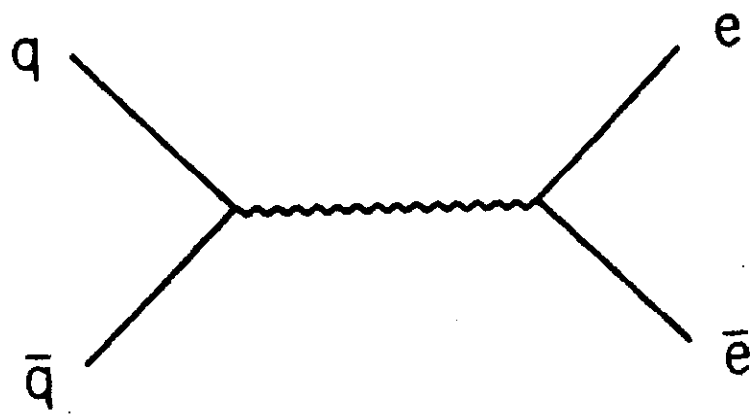


FIGURE 7

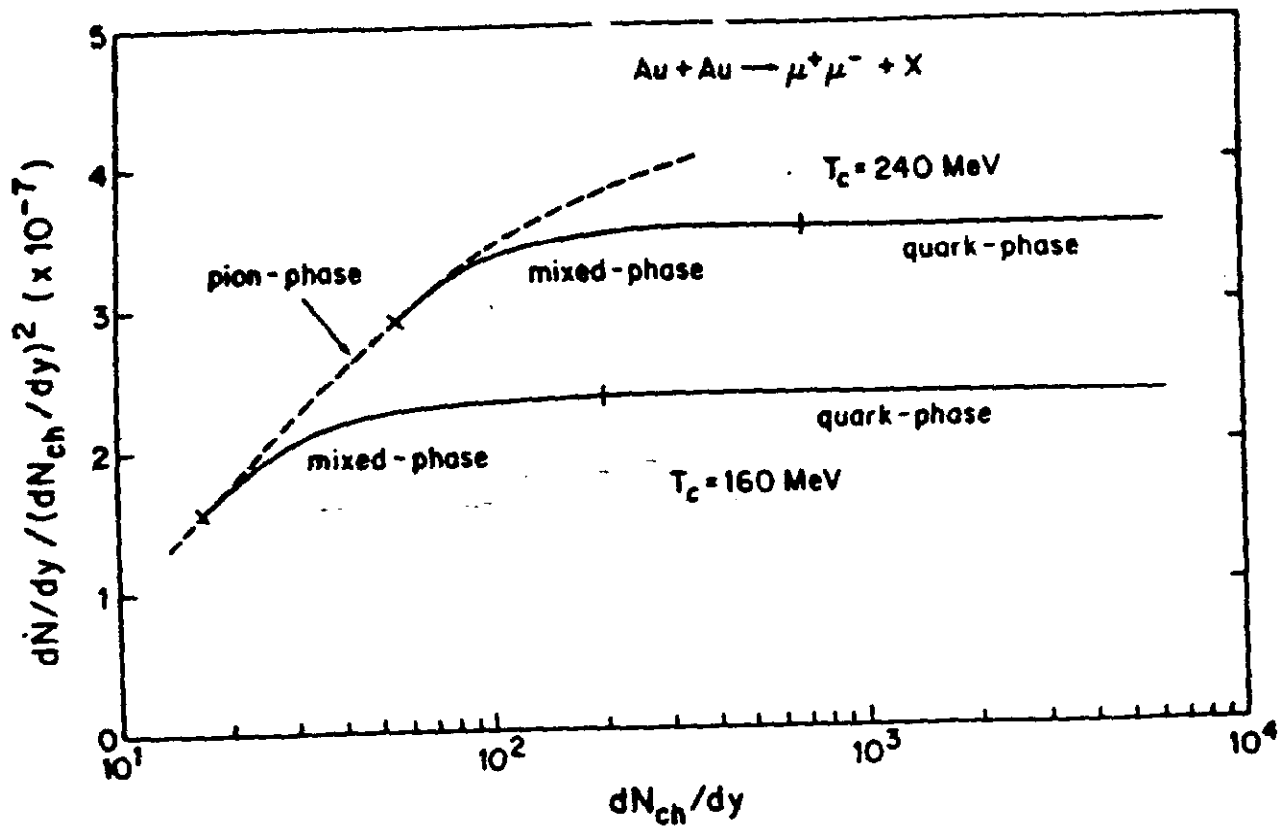


FIGURE 8

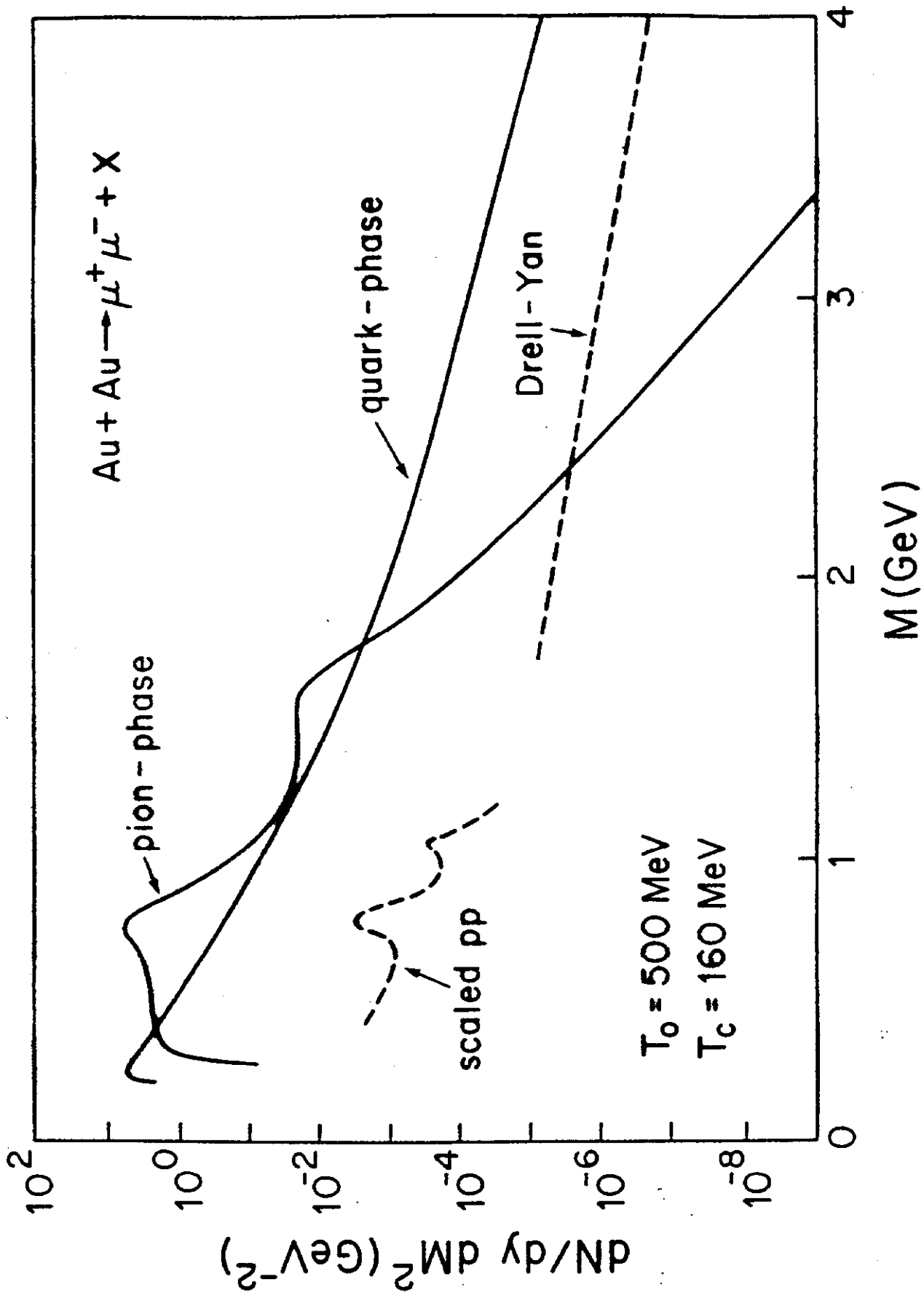


FIGURE 9 a

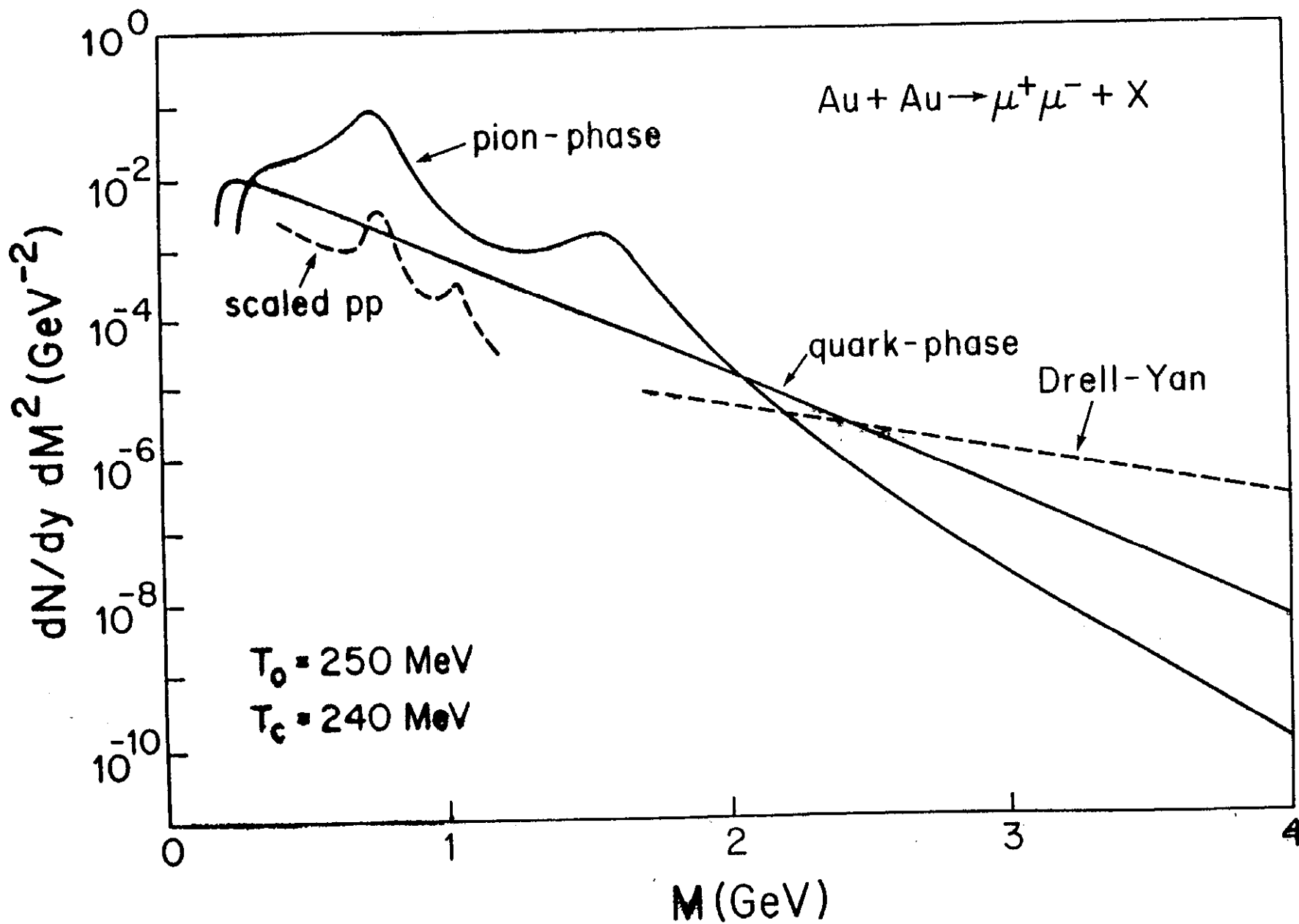


FIGURE 9 b

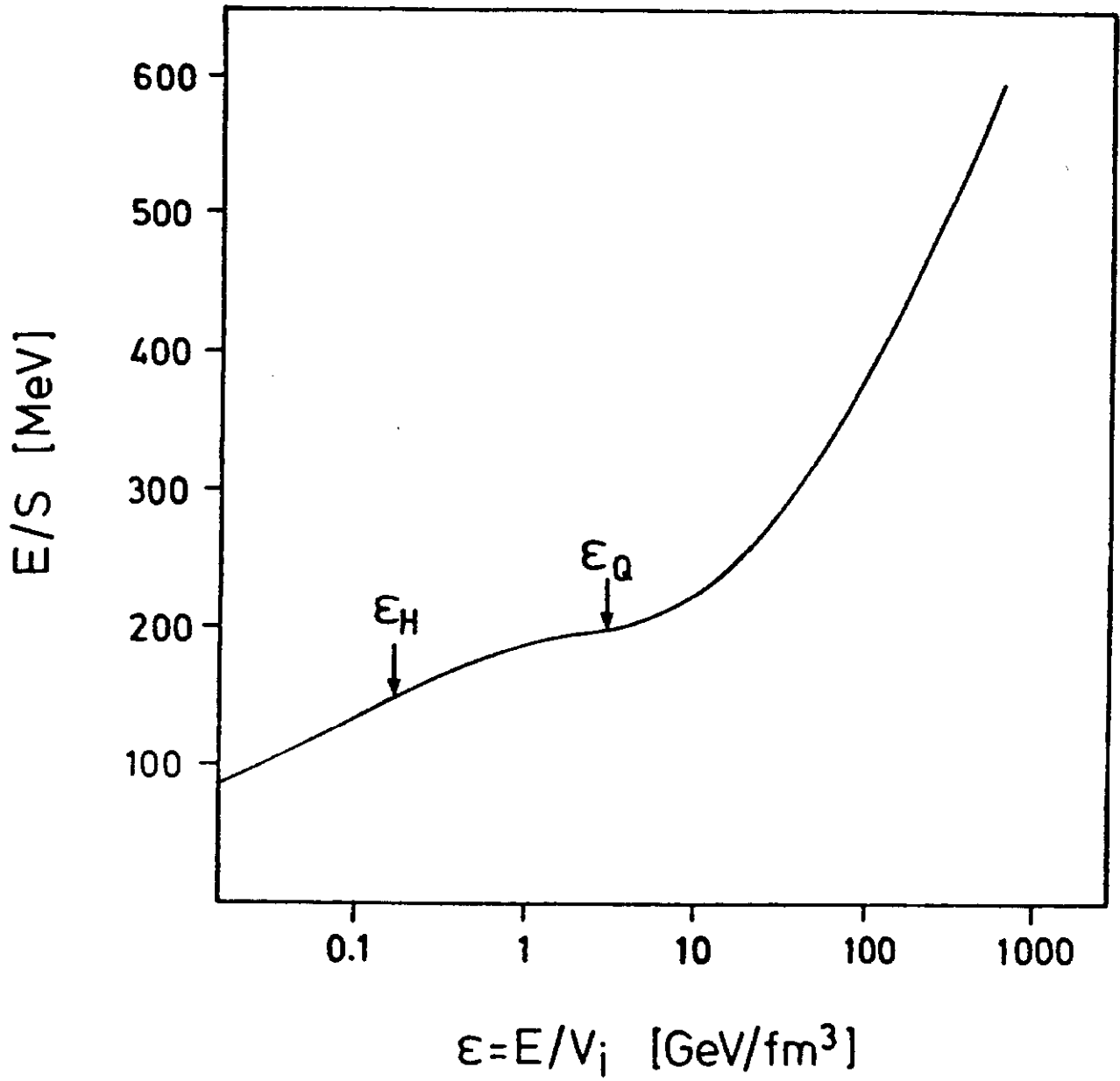


FIGURE 10

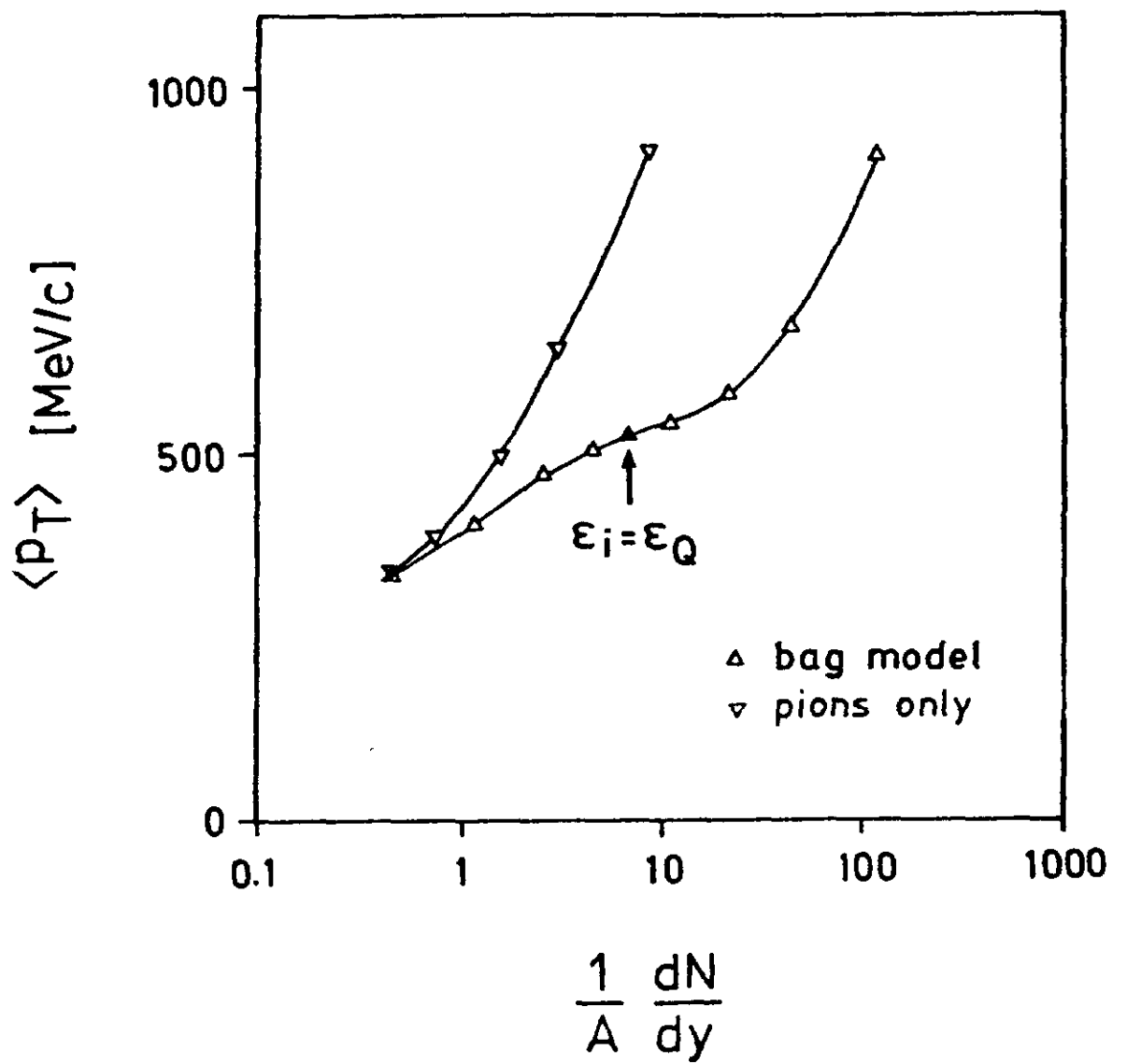


FIGURE 11

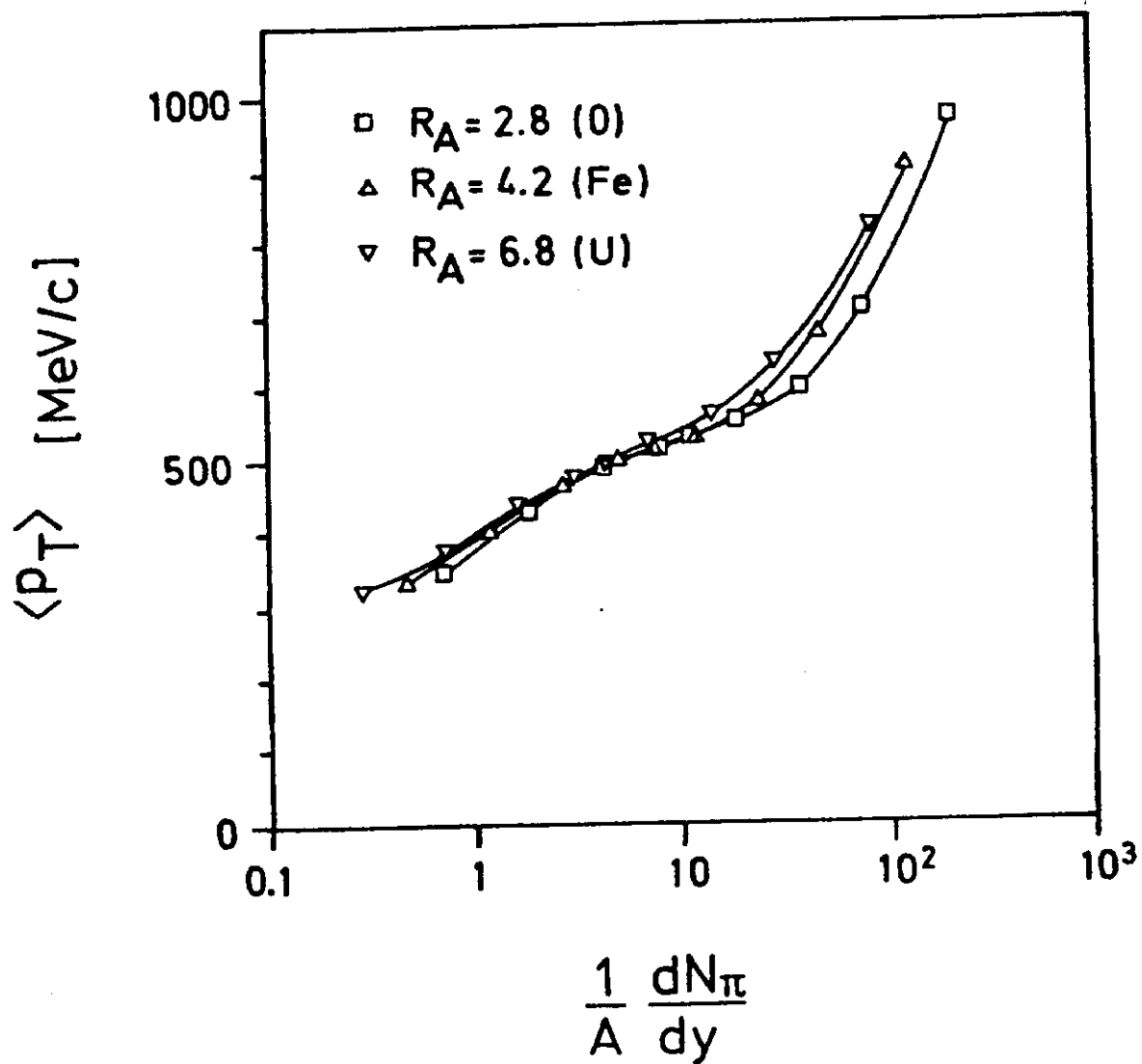


FIGURE 12

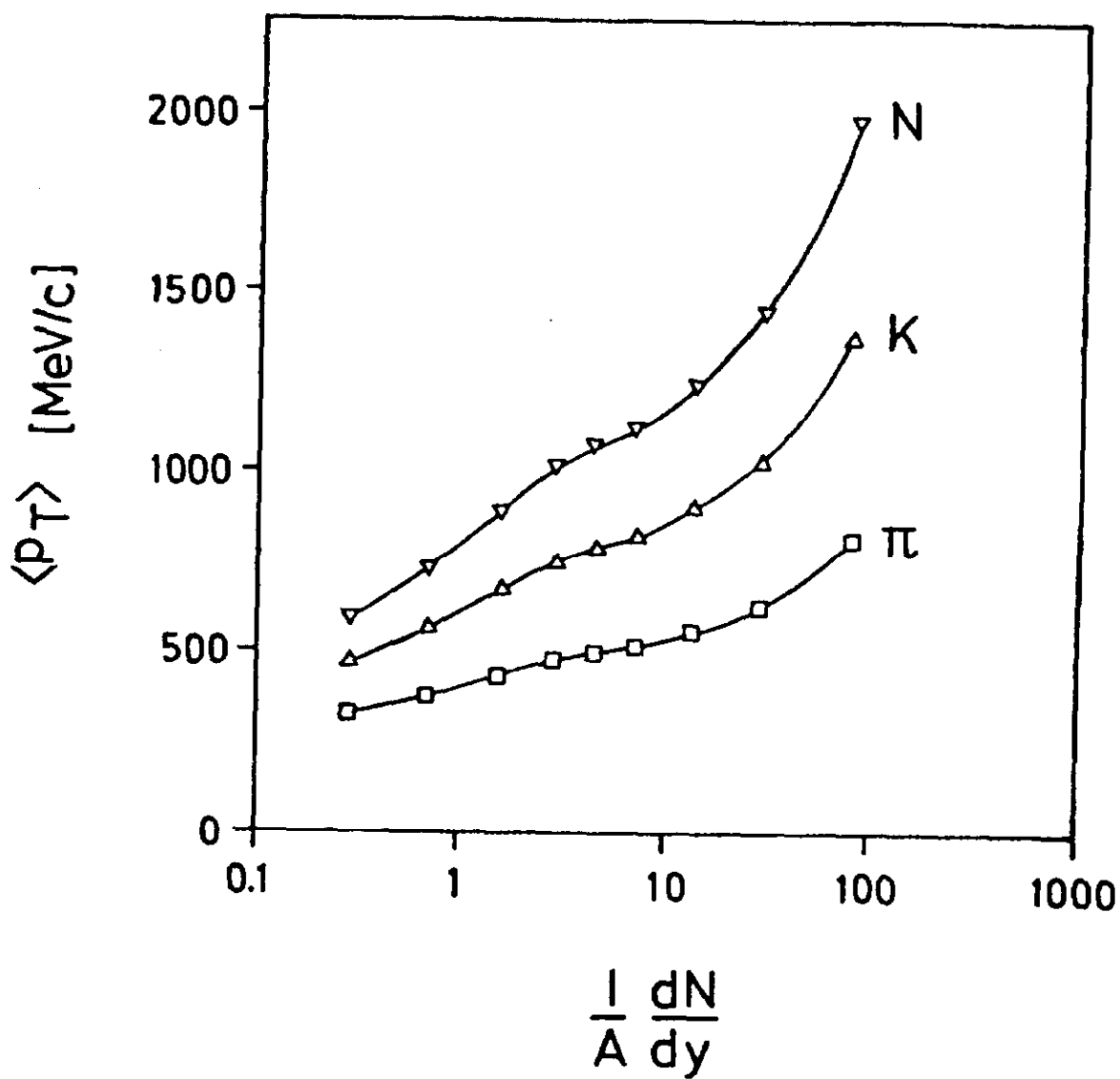


FIGURE 13

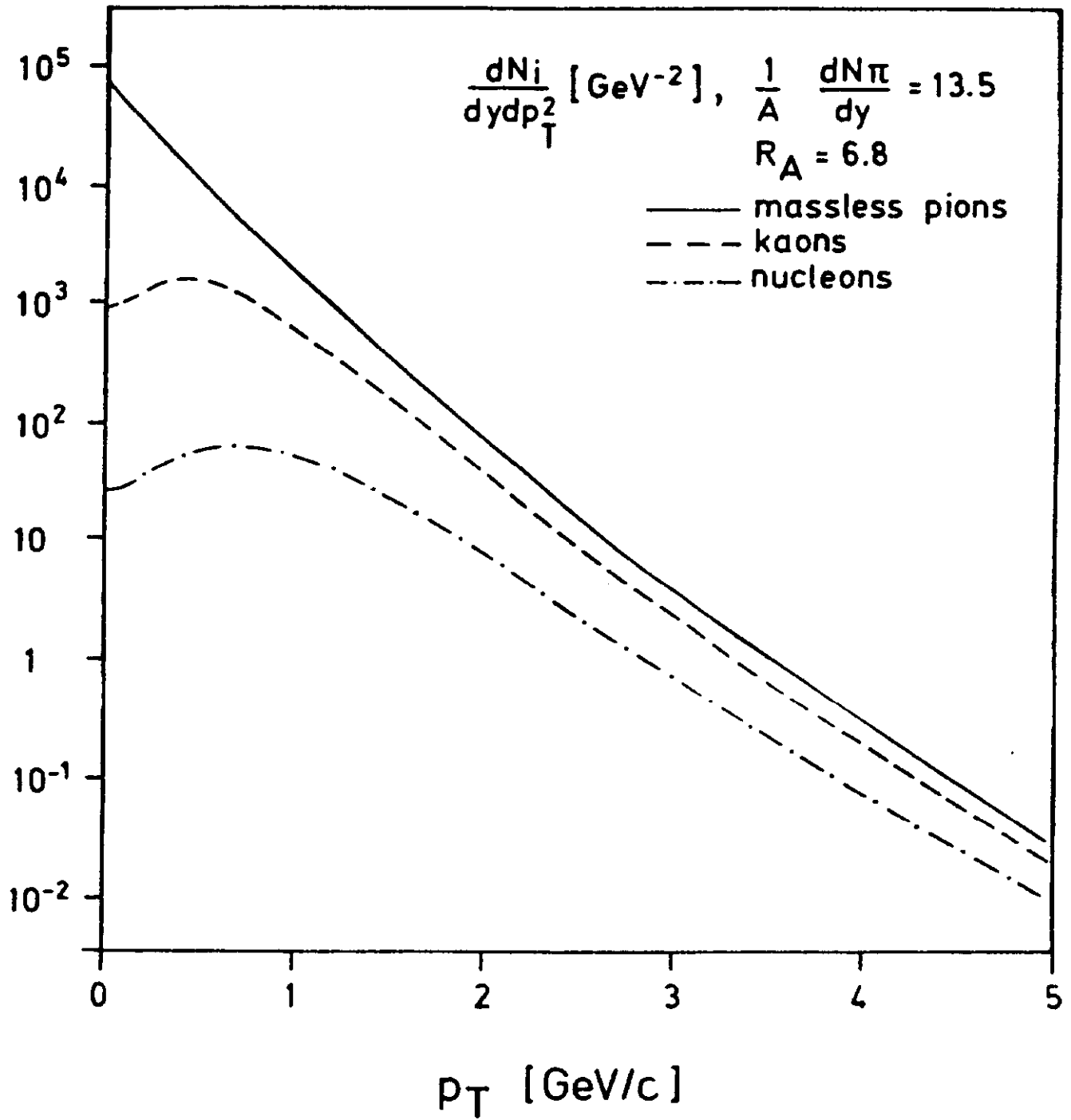


FIGURE 14

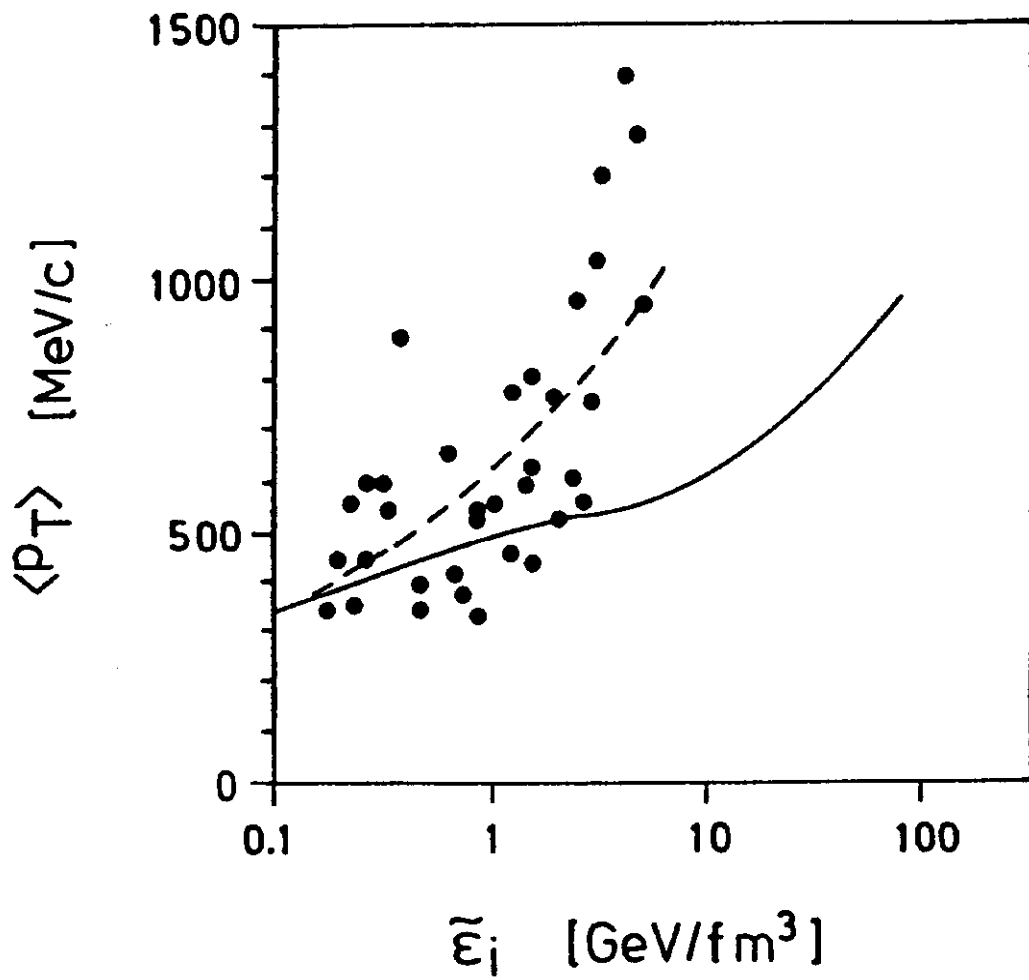


FIGURE 15

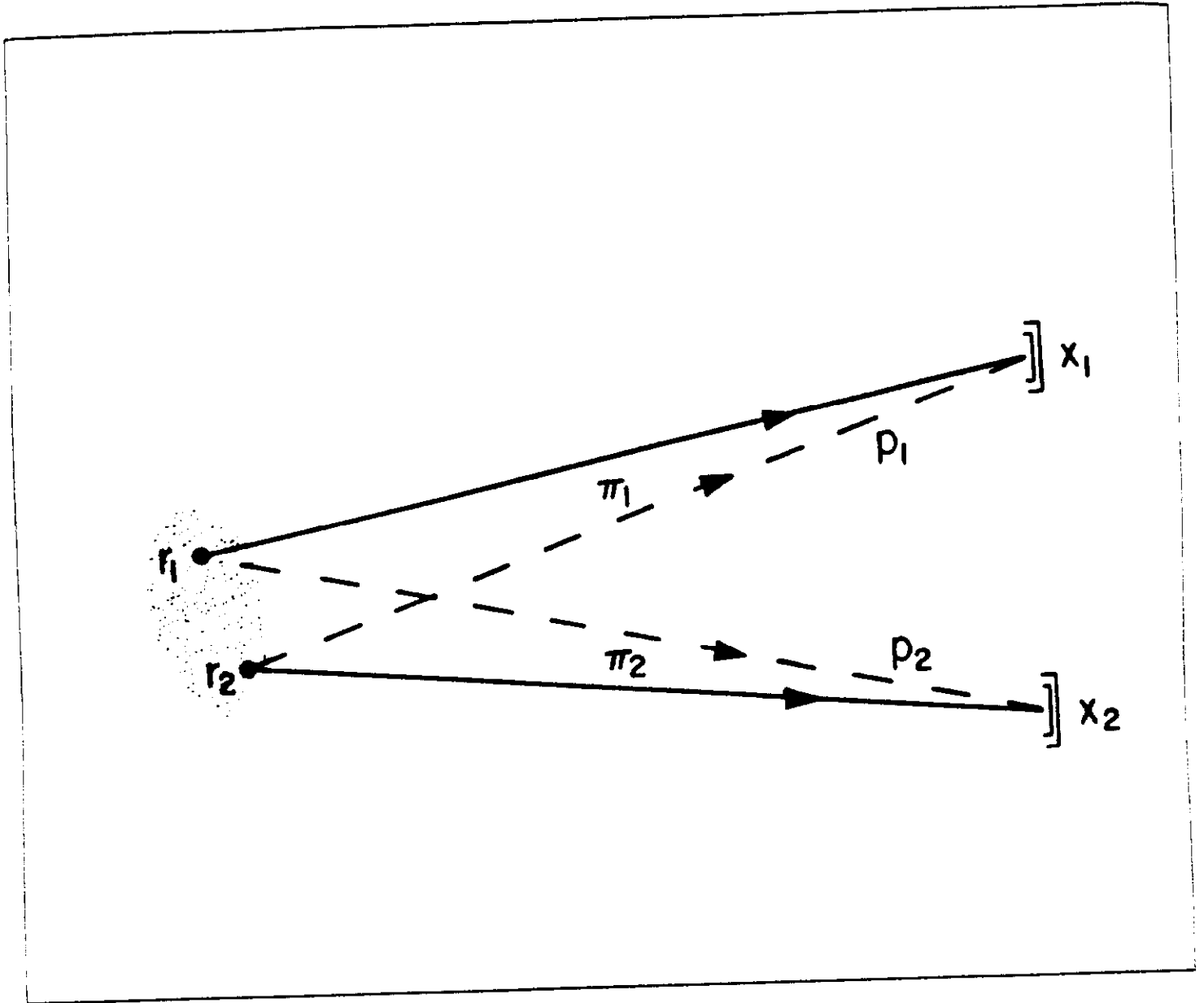


FIGURE 16

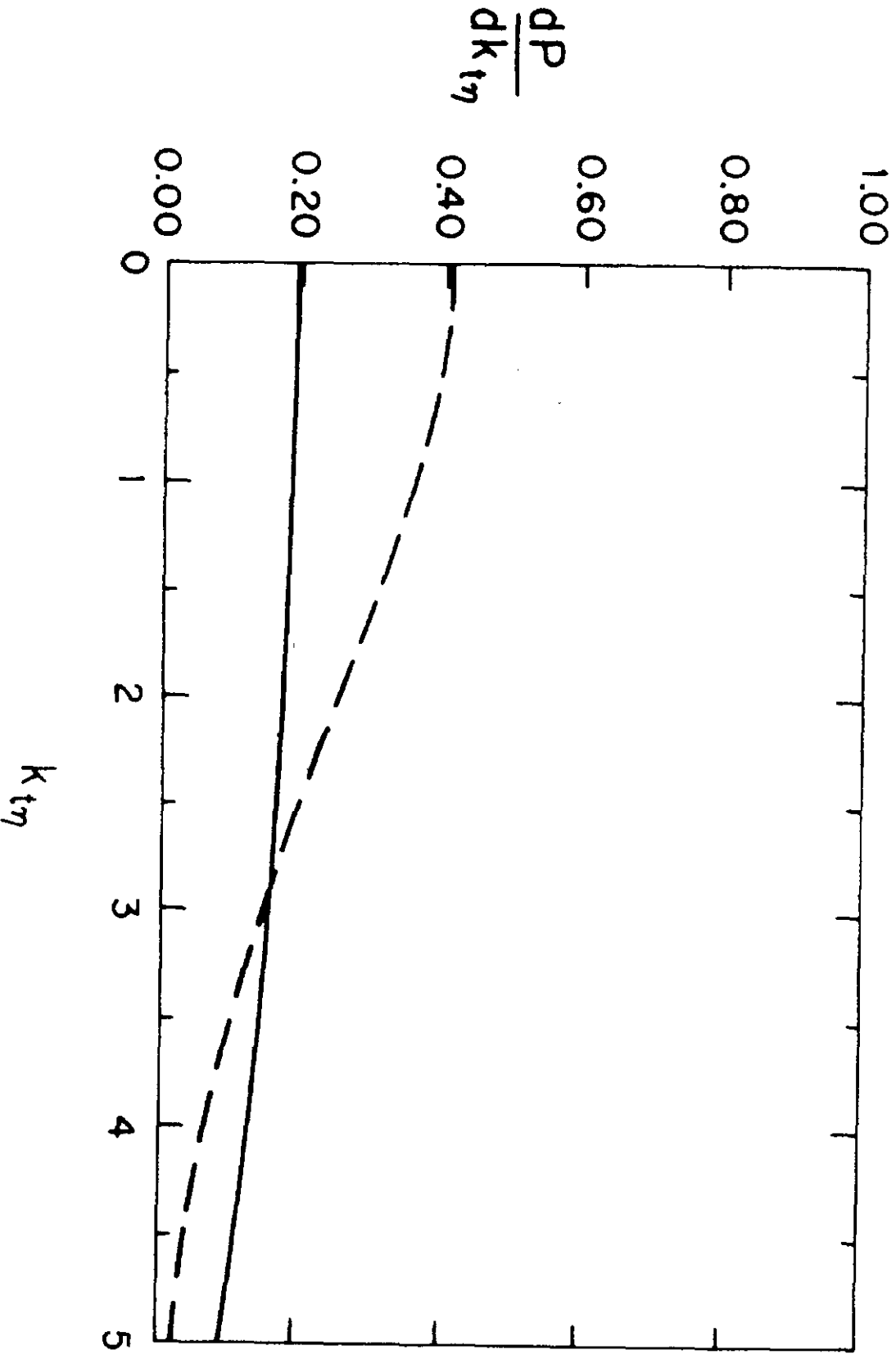


FIGURE 17 a

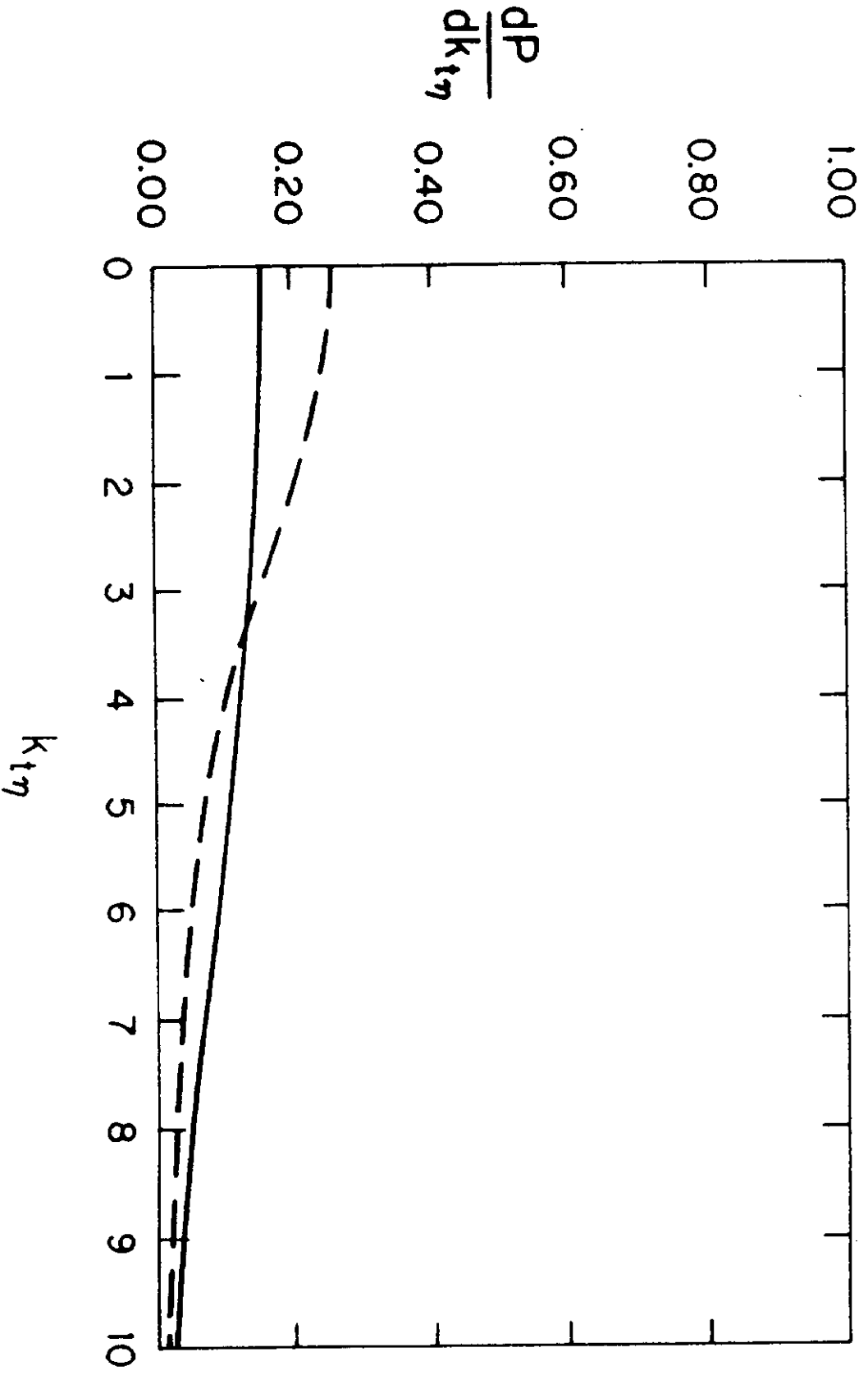


FIGURE 17 c

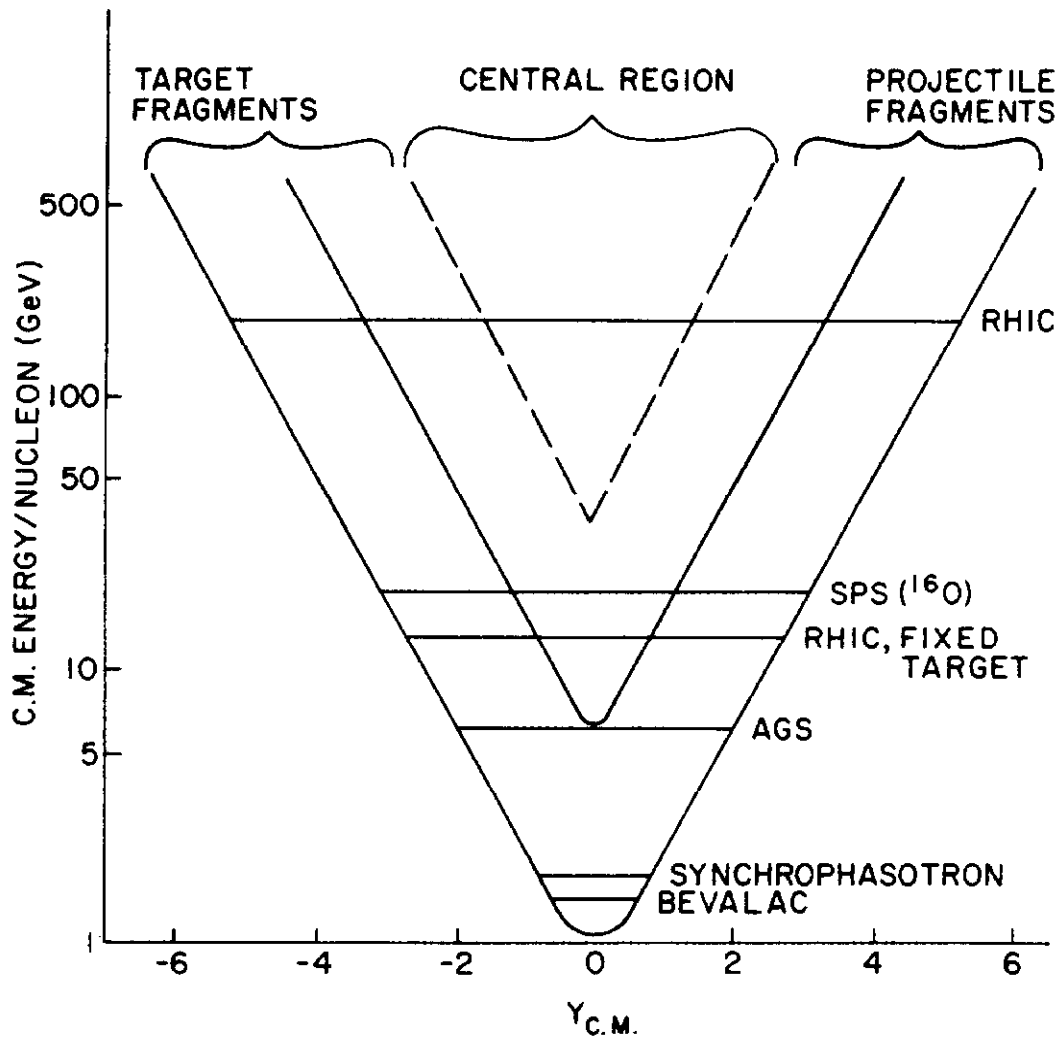


FIGURE 18